Blocking inflammasome activation caused by β-amyloid peptide (Aβ) and islet amyloid polypeptide (IAPP) through an IAPP mimic

Maryam Aftabizadeh[1,2,3], Marianna Tatarek-Nossol[2], Erika Andreetto[1], Omar El Bounkari[4], Markus Kipp[5], Cordian Beyer[6], Eicke Latz[7,8], Jürgen Bernhagen[4,9*], and Aphrodite Kapurniotu[1*]

[1]Division of Peptide Biochemistry, Technische Universität München, Emil-Erlenmeyer-Forum 5, D-85354 Freising (Germany); [2]Institute of Biochemistry and Molecular Cell Biology and [6]Institute of Neuroanatomy, RWTH Aachen University, Pauwelsstr. 30, 52074 Aachen (Germany); [3]Cancer Immunotherapeutics and Tumor Immunology, City of Hope Medical Center Duarte, 1500 East Duarte Road, Duarte, CA 91010-3000 (USA); [4]Chair of Vascular Biology, Institute for Stroke and Dementia Research, Klinikum der Universität München, Ludwig-Maximilians-University of Munich, 81377 Munich (Germany); [5]Department of Anatomy II, Ludwig-Maximilians-University of Munich, 80336 Munich (Germany); [7]Institute of Innate Immunity, University of Bonn, Biomedical Center, University of Bonn, Sigmund-Freud-Str. 25, 53127 Bonn (Germany); [8]University of Massachusetts Medical School, Division of Infectious Diseases & Immunology, 364 Plantation St., Worcester, MA 01605 (USA); [9]Munich Cluster for Systems Neurology (SyNergy), 81377 Munich (Germany).

Short title: Blocking inflammasome activity by an IAPP mimic

Key words: islet amyloid polypeptide; β-amyloid peptide; amyloid inhibitor; inflammasome activation; Alzheimer's disease; type 2 diabetes

***Corresponding authors:**

Prof. Aphrodite Kapurniotu, PhD

Division of Peptide Biochemistry

Technische Universität München (TUM)

Emil-Erlenmeyer-Forum 5, D-85354 Freising (Germany)

Tel. +49-8161-713542

E-mail: akapurniotu@wzw.tum.de

Prof. Jürgen Bernhagen, PhD

Chair of Vascular Biology

Institute for Stroke and Dementia Research (ISD)

Klinikum der Universität München

Ludwig-Maximilians-University (LMU) Munich

Feodor-Lynen-Straße 17, 81377 Munich, Germany

Tel.: +49-89 4400 - 46151

Fax: +49-89 4400 - 46010

E-Mail: juergen.bernhagen@med.uni-muenchen.de

Web: http://BernhagenLab.isd-muc.de

ABSTRACT

Inflammation in brain and pancreas is linked to cell degeneration and pathogenesis of both Alzheimer's-disease (AD) and type 2-diabetes. Inflammatory cascades in both tissues are triggered by the uptake of β-amyloid-peptide (Aβ) or islet-amyloid-polypeptide (IAPP) aggregates by microglial-cells (AD) or macrophages (T2D) and their insufficient lysosomal degradation. This results in lysosomal damage, caspase-1/NLRP3-inflammasome activation and release of interleukin-1β (IL-1β), a key pro-inflammatory cytokine in both diseases. Here we show that the inflammatory processes mediated by Aβ and IAPP aggregates in microglial cells and macrophages are blocked by IAPP-GI, a non-amyloidogenic IAPP mimic, which forms high-affinity soluble and non-fibrillar hetero-oligomers with both polypeptides. In contrast to fibrillar Aβ aggregates, non-fibrillar Aβ/IAPP-GI or Aβ/IAPP hetero-oligomers become rapidly internalized by microglial cells and targeted to lysosomes where Aβ is fully degraded. Internalization occurs via IAPP receptor-mediated endocytosis. Moreover, in contrast to IAPP aggregates, IAPP/IAPP-GI hetero-oligomers become rapidly internalized and degraded in the lysosomal compartments of macrophages. Our findings uncover a previously unknown function for the IAPP/Aβ cross-amyloid interaction and suggest that conversion of Aβ or IAPP into lysosome-targeted and easily degradable hetero-oligomers by hetero-association with IAPP mimics could become a promising approach to specifically prevent amyloid-mediated inflammation in AD, T2D or both diseases.

INTRODUCTION

Inflammatory processes in brain or pancreas play a central role in cell degeneration and in the onset and pathogenesis of Alzheimer's disease (AD) and type 2 diabetes mellitus (T2D)[1-4]. In fact, in AD it is becoming increasingly clear that inflammation and immune system-mediated actions, in particular those associated with innate immune pathways are main causative contributors to the neurodegenerative process, with microglia, the resident macrophage and a local innate immune cell of the brain, and inflammatory cytokines taking center stage[5-7]. Accordingly, a crucial event in brain inflammation in AD is the persistent activation of microglial cells by extracellular amyloid deposits, which mainly consist of fibrillar aggregates of the 40- to 42-residue β-amyloid peptide (Aβ40(42))[8-11]. Microglial cells then secrete inflammatory and neurotoxic factors, which induce a self-perpetuating, vicious cycle of aberrant inflammatory responses and neurotoxicity[1, 9, 10]. A key inflammatory cytokine driving this cycle that is released by activated microglial cells in response to Aβ-amyloid is interleukin-1β (IL-1β)[1, 8]. High IL1-β expression is found in microglial cells around amyloid plaques of AD patients and in AD disease-related animal models and increased levels of IL-1β have been detected in the cerebrospinal fluids (CSF) of AD patients[12-15]. Production of active IL-1β involves processing by caspase-1 that is activated by inflammasomes such as the NLRP3 (NOD-like receptor family, pyrin domain-containing 3) inflam-masome, a multi-protein complex that senses danger-associated molecular patterns (DAMPs)[16]. NLRP3 is a key guard of innate immunity and a major regulator of IL-1β and has been implicated in chronic inflammatory diseases[16]. Golenbock *et al.* showed that fibrillar Aβ42 aggregates represent a crucial inflammasome-activating class of DAMPs[17]. Exposure of microglial cells to Aβ42 aggregates activated NLRP3 leading to IL-1β secretion[17]. While the precise mechanism of Aβ aggregation and its link to cellular uptake is not entirely clear, it has been suggested that formation of β-sheet-rich aggregates is a prerequisite for Aβ42 uptake and cytotoxicity[18]. Thus, endocytosis or phagocytosis of Aβ42 aggregates by microglia likely causes lysosomal dysfunction and cathepsin B release into the cytosol, resulting in NLRP3/caspase-1 activation[17]. Importantly, the crucial role of the NLRP3 inflammasome in AD pathology has also been demonstrated in an *in vivo* mouse models of AD[15, 19, 20].

In T2D, amyloid plaques consisting of fibrillar aggregates of islet-amyloid polypeptide (IAPP) are present in the pancreas of >95% of patients[21]. IAPP is a 37-residue peptide hormone synthesized and secreted from pancreatic β-cells together with insulin[21, 22]. In its soluble form, IAPP monomers act as a regulator of glucose homeostasis via binding to neuronal receptors mainly located in the central nervous system[21, 23, 24]. IAPP aggregates, however, activate NLRP3 and caspase-1, likely via lysosomal perturbation, to trigger IL-1β release from macrophages which infiltrate pancreatic islets and adipose tissue, thus affecting insulin function and inducing inflammation and apoptotic β-cell death[25-27]. In addition, increased IL-1β levels have been found in pancreatic islets of mice transgenic for human IAPP where they colocalize with IAPP amyloid and infiltrated pancreatic macrophages, suggesting a direct link between IAPP-mediated NLRP3 inflammasome activation and T2D pathology[25, 27, 28].

Thus, Aβ and IAPP aggregates are key players in microglia- or macrophage-mediated inflammatory processes underlying cell degeneration in both AD and T2D by activation of the caspase 1/NLRP-3 axis[28, 29]. Emerging epidemiological, pathophysiological, and molecular evidence suggests that beyond their inflammation link, AD and T2D share other common features as well[30]. For instance, AD patients have a strongly increased risk for T2D and *vice versa*, while amyloid deposits of both Aβ and IAPP are present in brain and pancreas of both AD and T2D patients[30-33]. Compounds targeting protein aggregation and related inflammatory cascades in both diseases could thus lead to novel therapeutic concepts targeting the pathogenesis of both diseases[28, 29, 33, 34].

The sequences of Aβ and IAPP share 50% similarity and 25% identity and, importantly, the two polypeptides are able to cross-interact[35, 36]. In particular, Aβ fibrils have been shown to accelerate IAPP amyloidogenesis, whereas high-affinity interactions between non-fibrillar Aβ and IAPP species result in soluble, non-fibrillar Aβ/IAPP hetero-oligomers, which lead to suppression of amyloid self-assembly of both polypeptides[35-37]. Of note,, the non-amyloidogenic IAPP analog [(N-Me)G24, (N-Me)I26]-IAPP (IAPP-GI) and related IAPP mimics are potent inhibitors of cytotoxic self-assembly of both Aβ40(42) and IAPP[35, 37-40]. In fact, IAPP-GI binds prefibrillar IAPP or Aβ40(42) species with high affinity and sequesters them from their cytotoxic self-assembly pathways in form of soluble, non-fibrillar and non-cytotoxic hetero-oligomers[35, 37, 38].

Against this background, we hypothesized that IAPP mimics such as IAPP-GI could represent a novel compound class targeting protein aggregation and inflammatory cascades in AD and T2D. To test this hypothesis, we probed the effect of IAPP-GI in amyloid-triggered microglial and macrophage activation, studying its effect on uptake, inflammasome activation, myeloid cell amyloid load, and lysosomal integrity. We also asked whether microglial cells express IAPP receptors and how they contribute to IAPP-GI-mediated inflammasome attenuation.

RESULTS AND DISCUSSION

The cross-amyloid inhibitor IAPP-GI prevents Aβ and IAPP aggregate-induced NLRP3 inflammasome activation in microglial cells and macrophages. We studied whether IAPP-GI is able to interfere with the inflammatory cascades mediated by Aβ40, Aβ42 and IAPP aggregates in mouse BV-2 microglial cells, immortalized peritoneal macrophages, and bone marrow-derived macrophages (BMDMs).

We first asked whether fibrillar aggregates of Aβ40 induce IL-1β release in an NLRP3-dependent manner from BV-2 microglia in a similar manner as reported for Aβ42 aggregates[17]. The BV-2 microglial cell line is derived from C57/BL6 mice and widely used, as it is a suitable substitute for primary microglial cells[41, 42]; in addition, it has previously been applied for studying the effects of Aβ42[17, 43]. BV-2 cells were primed with LPS, representing a surrogate signal 1 for sterile inflammasome priming, and incubated with aged fibrillar Aβ40 (*called herein*: fibrillar Aβ40, fAβ40 or aged Aβ40), verified to be of fibrillar nature by ThT binding assay[17, 35]. Inflammasome activation was assessed by quantifying caspase-1 activity in cell lysates using the cell-permeable probe FAM-YVAD-fmk (FLICA) and confirmed by detection of auto-proteolytic production of caspase-1 fragment p10 by Western blot[17]. In fact, aged Aβ40 strongly activated caspase-1 as indicated by comparison with LPS priming alone or LPS followed by ATP stimulation, a known second hit trigger of NLRP3 (**Figure 1A**, **Supplementary Figures S1 and S2**). As expected, a solution containing freshly dissolved Aβ40 and consisting mainly of non-fibrillar Aβ40 species as confirmed by ThT binding did not activate caspase-1 (**Supplementary Figure S3** and data not shown)[17, 35].

Next, the effect of IAPP-GI on Aβ40-mediated caspase-1 activation as measured by FLICA assay was determined following incubation of the BV-2 cells with an aged mixture of Aβ40 with IAPP-GI (1/1), a ratio that had previously been demonstrated to convey complete inhibition of Aβ or IAPP fibrillogenesis[35, 38] and that was used here and for all subsequent inhibition experiments in our study. The stimulatory effect that Aβ40 aggregates have on caspase-1 activity was abrogated when Aβ40 aging was performed in the presence of IAPP-GI (**Figure 1A**, **Supplementary Figure S2**). Of note, Aβ40 amyloid self-assembly also was blocked in the presence of IAPP-GI as previously reported (**Supplementary Figure S3B**)[35].

Aged Aβ40 preparations also significantly activated caspase-1 in the absence of LPS priming and IAPP-GI was able to fully inhibit this effect (**Figure 1B**). A priming step by classical NFκB-activating triggers such LPS or TNF-α is typically required for transcription of the IL-1β precursor protein and to some extent, especially when protein concentrations are limiting, for induction of the NLPR3 protein subunits, while the caspase-1 activity *per se* does not require a signal 1-based priming step. We assume that BV-2 microglial cells express non-limiting concentrations of NLRP3 at baseline; moreover, Aβ has been suggested to exhibit DAMP-like activities via the CD14/TLR axis (e.g.[44]). Of note, these experiments confirmed a similar effect for fibrillar Aβ42, corroborating the earlier studies by Halle et al.[17], and showed that IAPP-GI (1/1) coincubation during the fibrillation process fully blocked caspase 1 activation by either Aβ40 or Aβ42 (**Figure 1B**). The observed caspase-1-activating activity of Aβ40 was somewhat higher than that of Aβ42, an effect likely due to the fact that the experimental aggregation/fibrillation conditions applied in our study were mainly optimized for Aβ40[35].

To verify the direct link of the above effects to NLRP3 activity, aged Aβ40 versus the mixture of aged Aβ40 with IAPP-GI (1/1) was applied to immortalized peritoneal macrophages (PMs) derived from wild-type (WT) or *Nlrp3*-deficient mice and caspase-1 activation was measured by FLICA assay[27]. A complete lack of caspase-1 activity in the *Nlrp3*$^{-/-}$ macrophages was observed, suggesting that Aβ40(42) aggregate-mediated caspase-1 activation in macrophages that is blocked in the presence of IAPP-GI depends on the presence of NLRP3 (**Figure 1C**).

Importantly, the observed effects on caspase-1 activation were accompanied by a corresponding regulation of IL-1β production. Stimulation of LPS-primed BV-2 microglial cells with aged fibrillar Aβ40 resulted in substantially enhanced IL-1β release up to 500 pg/ml as shown by ELISA-based IL-1β quantification in the supernatants. In comparison, when BV-2 cells were treated with Aβ40 co-aged in the presence of IAPP-GI (1/1), the increase in IL-1β levels was significantly suppressed (**Figure 1D**). Aβ40-triggered IL-1β release was even more pronounced in immortalized PMs isolated from wildtype mice (PM-WT). As in microglial cells, this effect was significantly attenuated when Aβ40 was aged in the presence of IAPP-GI and comparative analysis in *Nlrp3*$^{-/-}$ PMs confirmed the dependence on NLRP3 activation (**Figure 1D**).

Because IAPP aggregates (*termed herein:* fibrillar IAPP, fIAPP, or aged IAPP) also have been shown to trigger IL-1β secretion from microglial cells and to activate the NLRP3 inflammasome to produce mature IL-1β in LPS-primed bone marrow-derived macrophages (BMDMs) and dendritic cells, we asked whether IAPP may activate caspase-1 in BV-2 cells and whether this effect can be blocked by IAPP-GI[27, 45]. Aged IAPP solutions mainly consisting of fibrillar IAPP assemblies but not aged mixtures of IAPP co-incubated with IAPP-GI (1/1) activated caspase-1 in BV-2 cells as determined by FLICA assay and caspase-1 p10 processing and triggered IL-1β release from BV-2 cells (**Figure 1A**, **Supplementary Figure S2,** and **Figure 1D**). The inhibitory effect of IAPP-GI on IAPP fibrillogenesis was confirmed by the ThT binding assay (**Supplementary Figure S4A**).

Although lower in magnitude, similar caspase-1 effects were seen in unprimed BV-2 cells (**Figure 1B**). Furthermore, aged fibrillar IAPP was applied to immortalized peritoneal macrophages derived from WT or *Nlrp3*-deficient mice and its effect compared with that of aged IAPP/IAPP-GI mixtures. IAPP but not IAPP/IAPP-GI mixtures activated caspase-1 and triggered IL-1β release in WT cells, whereas caspase-1 activation and IL-1β secretion was ablated in *Nlrp3*$^{-/-}$ macrophages, confirming NLRP3 dependence (**Figure 1C** and **D**). To further confirm the inhibitory effect of IAPP-GI on IAPP amyloid-induced NLRP3 activation, primary BMDMs following differentiation with macrophage colony-stimulating factor (M-CSF) were studied (for macrophage phenotype verification see **Supplementary Figure S4B**). IAPP also caused a significant activation of caspase-1 in these cells, whereas in the presence of IAPP-GI, activation of caspase-1 by fibrillar IAPP was abrogated (**Figure 1E**). These results provided evidence that IAPP aggregate-mediated caspase-1 activation in microglial cells and macrophages was potently blocked by IAPP-GI and depended on NLRP3 activity.

IAPP-GI (and native IAPP) suppresses Aβ-mediated lysosomal leakage and colocalizes with Aβ in lysosomal compartments. The inability of lysosomes to efficiently degrade Aβ amyloid aggregates following endocytosis/phagocytosis has been shown to underlie inflammasome activation by Aβ in immortalized primary microglial cells[17, 46], involving lysosomal dysfunction, cytosolic exposure of cathepsin B, NLRP3 activation, and IL-1β release[17]. Of note, lysosomal dysfunction is linked to various features of AD pathogenesis[17, 47]. To investigate whether the inhibitory effect of IAPP-GI on Aβ-induced

activation of caspase-1 and IL-1β release would involve suppression of Aβ-mediated lysosomal leakage, we measured intracellular cathepsin B activity in BV-2 cells using a fluorescent, cell-permeable cathepsin B substrate[17]. In fact, significantly enhanced cathepsin B activity was only detected in cells treated with aged, fibrillar, Aβ40 alone, but not in those cell incubations treated with vehicle or Aβ40/-IAPP-GI mixtures (**Figure 2A**). Lysosomal cathepsin B leakage was confirmed by Western blot of cathepsin B protein levels in isolated LAMP-1+ lysosomal fractions from BV-2 cells which revealed strongly reduced amounts of cathepsin B in lysosomal fractions of cells treated with aged fibrillar Aβ40 as compared to fractions from control cells or cells treated with Aβ40/IAPP-GI mixtures (**Figure 2B** and **2C**). These results suggested that inhibition of NLRP3/caspase-1 activation by IAPP-GI correlates with a suppression of Aβ aggregate-mediated lysosomal leakage.

Two mechanisms could account for the observed strong inhibitory effect of IAPP-GI on Aβ-mediated lysosomal damage and caspase-1 activation: (i) nonfibrillar Aβ/IAPP-GI hetero-oligomers become internalized by microglial cells and targeted to lysosomes where they are more efficiently degraded than the aggregates of Aβ or (ii) nonfibrillar Aβ/IAPP-GI hetero-oligomers do not enter microglial cells but their formation sequesters Aβ from its self-assembly pathway, reducing the amount of Aβ that is subjected to phagocytosis/uptake.

To address the two scenarios, we first investigated whether Aβ40/IAPP-GI hetero-oligomers become internalized and targeted to lysosomes of BV-2 cells. Cells were incubated (16 h) with synthetic N^{α}-amino-terminal fluorescently labeled peptides (Fluos-Aβ40, Rhodamin-Aβ40, or Fluos-IAPP-GI) or 1/1 mixtures thereof and internalization and lysosomal accumulation were studied by confocal laser-scanning microscopy, using LysoTracker Red to co-stain for lysosomes/late endosomes (**Figure 3**) Confirming prior findings[17, 46], we noted strong lysosomal targeting of Fluos-Aβ40 alone (**Figure 3A**). Interestingly, Fluos-IAPP-GI alone was also internalized and targeted to lysosomal compartments (**Figure 3B**). Importantly, lysosomal targeting of Fluos-Aβ40 was also observed when a 1/1 mixture with unlabeled IAPP-GI was added to the cells (**Figure 3C**). This experiment also was in line with the notion that most, if not all, complexes taken up intracellularly, colocalized with lysosomal compartments. Moreover, incubating BV-2 cells with a mixture of both peptides in their labeled forms, i.e. Rhodamin-Aβ40 and Fluos-IAPP-GI, clearly verified the lysosomal co-localization of both peptides,

confirming co-trafficking of Aβ40/IAPP-GI complexes (**Figure 3D**). As the apparent K_d of the Aβ40/IAPP-GI interaction *in vitro* has been shown to be ~48nM, most of the Aβ40 or IAPP-GI molecules in the mixture (200 nM each) should be present within hetero-oligomers[35]. To further confirm and quantify these findings, aged fibrillar Aβ40, Aβ40/IAPP-GI mixtures (1/1), or IAPP-GI alone were incubated with BV-2 cells, lysosomes isolated after 0, 2 and 16 h, and lysosomal Aβ40 quantified by Western blot. Lysosomes at 0 h did not contain any detectable Aβ40, whereas large amounts of Aβ40 were found at 2 and 16 h, when cells were incubated with Aβ40-alone aggregates (**Figure 3E**). These results were consistent with established lysosomal targeting kinetics and the previously suggested slow and incomplete degradation process of fibrillar Aβ40 aggregates[17, 35, 46, 48]. Importantly, only small quantities of Aβ40 were detected in lysosomes of cells treated with Aβ40/IAPP-GI mixtures consistent with a nearly complete disappearance of Aβ40 in the context of Aβ40/IAPP-GI complexes (**Figure 3E**). In addition, detection with an anti-IAPP antibody confirmed that IAPP-GI was co-targeted to the lysosomes (**Figure 3E**). As expected, non-aged (non-fibrillar) Aβ40 became rapidly degraded in the lysosomes and did not cause caspase-1 activation (**Supplementary Figure S5**)[17]. The ability of lysosomal enzymes to degrade Aβ40 in the context of Aβ40/IAPP-GI hetero-oligomeric complexes was further supported by Western blot and MALDI-mass spectrometry analysis of their *in vitro* incubations with BV-2 lysosomal extracts or purified cathepsin B (**Supplementary Figure S6**). In aggregate and together with the cathepsin B leakage data of Figure 2, these results suggest that Aβ40/IAPP-GI complexes are efficiently targeted to the lysosomal compartment, where Aβ40 is rapidly degraded. They also indicate that it is unlikely that appreciable portions of the complexes are released from the lysosomal compartment.

Next, IAPP-GI was added to an already aged fibrillar Aβ40 solution (1/1) and following incubation with BV-2 cells, lysosomal contents were analyzed for Aβ40 by Western blot analysis. Similar Aβ40 contents were found in the lysosomal extracts of cells treated with fibrillar Aβ40 alone or the mixture (**Figure 4A**). These results support the suggestion that interaction of IAPP-GI with nonfibrillar Aβ species is required for the above-observed uptake effect and/or efficient lysosomal degradation of Aβ. In addition, probing the lysosomal degradation rate of aged mixtures of Aβ40 with glucagon (1/1) confirmed that a sequence-specific interaction underlies the enhanced uptake and lysosomal degradation

of Aβ in the presence of IAPP-GI (**Figure 4B**). Moreover, the effects of two well-known inhibitors of Aβ aggregation, the pentapeptide LPFFD and epigallocatechin gallate (EGCG), were studied[49, 50]. Of note, Aβ40 aggregate-triggered caspase-1 activation was not significantly reduced in mixtures of Aβ40 with LPFFD or EGCG (**Supplementary Figure S7**; p=NS and p=0.06 versus Aβ40 aggregate-alone). Moreover, no reduction in lysosomal Aβ40 content was observed in cells treated with EGCG/Aβ40 or LPFFD/Aβ40 mixtures as compared to fibrillar Aβ40 aggregates alone (**Figure 4C** and **D**). By contrast, in lysosomes of cells treated with EGCG/Aβ40 mixtures, large amounts of Aβ40-containing assemblies were found consistent with formation of EGCG/Aβ40 hetero-assemblies as previously reported (**Figure 4D**)[50]. In aggregate, these results suggested that the inhibitory effect of IAPP-GI on Aβ amyloid self-assembly is not the main reason for the low amount of Aβ aggregates found in lysosomes of microglial cells treated with Aβ40/IAPP-GI mixtures.

To further dissect the effects of IAPP-GI related to its inhibitory effect on Aβ aggregation from the other possible mechanisms, we next studied the effect of mixtures of Aβ40 with rat IAPP (rIAPP) on lysosomal degradation of Aβ40 and on Aβ40-mediated caspase-1 activation. rIAPP, a natively occurring soluble and non-amyloidogenic analog of IAPP which differs from IAPP in 6 out of 37 residues, is a weak inhibitor of Aβ40 self-assembly although it binds Aβ40 with high affinity (data not shown and[35]). On the other hand, rIAPP is the most potent natively occurring human IAPP receptor agonist[51, 52]. Importantly, substantially reduced amounts of Aβ40 were found in the lysosomes of cells treated with aged Aβ40/rIAPP (1/1) mixtures as compared to aged Aβ40 alone and caspase-1 activity was completely suppressed (**Figure 4E, F**). These results supported the hypothesis that microglial uptake and degradation of hetero-assemblies of Aβ with IAPP-GI or rIAPP account for the inhibitory effects of the two IAPP analogs on Aβ-mediated caspase-1 activation.

The above results and the fact that IAPP-GI is a mimic of a non-amyloidogenic IAPP conformer, prompted us to study the effects of non-fibrillar IAPP on Aβ40-mediated caspase-1 activation and Aβ40 degradation as well. Importantly, no caspase-1 activation was found in BV-2 cells treated with aged Aβ40/IAPP (1/1) mixtures whereas aged solutions of Aβ40 or IAPP alone strongly activated caspase-1 (**Figure 4G**). Moreover, dramatically reduced concentrations of lysosomal Aβ40 and IAPP were found in cells treated with aged Aβ40/IAPP (1/1) mixtures as compared to cells treated with aged fibrillar

solutions of each of the peptides alone (**Figure 4H**). These results supported the suggestion that, similarly to Aβ/IAPP-GI hetero-oligomers, non-fibrillar Aβ/IAPP hetero-oligomers are targeted to lysosomes, where both components are efficiently degraded, thus preventing lysosomal damage and inflammasome activation.

Aβ/IAPP-GI hetero-oligomers bind to a microglial IAPP receptor and are internalized by receptor-mediated endocytosis. To understand the uptake mechanism of Aβ/IAPP-GI (or Aβ/IAPP) hetero-oligomers, we quantified extracellular Aβ40 in supernatants of BV-2 cells treated with aged Aβ40 versus aged Aβ40/IAPP-GI (1/1) mixtures at time points of 2 min and 16 h, i.e. very early and late time points of the uptake process (*see* **Figure 3**). Intriguingly, Aβ40 in the context of Aβ40/IAPP-GI hetero-assemblies, nearly quantitatively disappeared from the cell supernatant as early as 2 min after addition of the mixture to the cells (**Figure 5A**). By contrast, substantial amounts of Aβ40 were present in the extracellular space at this time point in the incubations of aged Aβ40 alone (difference in internalization rate: 6-fold). This difference leveled off after 16 h, suggesting that uptake of fibrillar Aβ40 aggregates by microglial cells occurs slower than uptake of Aβ40/IAPP-GI hetero-oligomers (**Figure 5B**). These findings argued for rapid, receptor-mediated, endocytosis of the Aβ/IAPP-GI hetero-assemblies. To substantiate this notion, we inhibited the clathrin-mediated endocytosis (CME) pathway by applying a combination of the inhibitors monodansylcadaverine (MDC) and Dynasore and examined the early phase (2-60 min) of Aβ40 uptake in the context of its hetero-assembly with IAPP-GI versus aged Aβ40 alone. Monodansylcadaverine specifically inhibits CME, while Dynasore, an inhibitor of dynamin-driven vesicle formation processes, not only blocks CME, but also other dynamin-dependent uptake processes including caveolin-dependent and -independent pathways[53, 54]. Aβ40 levels in the cell lysates were quantified and the result showed that the endocytosis inhibitors significantly reduced uptake of Aβ40 at the 60 min time point, when Aβ40 was applied as hetero-oligomer with IAPP-GI, but not when aged Aβ40 alone was applied (**Figure 5C** and **Supplementary Figure S8**). The experiments suggested that microglial uptake of IAPP-GI/Aβ40 hetero-oligomers appeared to occur by receptor-mediated endocytosis and we next tested this notion further.

Due to their multiple roles in homeostasis and inflammation, microglial cells express a diverse range of cell membrane receptors including PRRs and receptors for cytokines, neurotransmitters, and neuropeptide hormones[55]. We asked whether the BV-2 microglial cells also express a functional receptor for IAPP. IAPP receptors are heterodimeric receptors present in various brain regions and consist of a calcitonin receptor (CTR) chain and one of three different receptor activity-modifying proteins (RAMPs) resulting in IAPP receptors AMY1, AMY2 and AMY3[23]. We first tested equilibrium binding of radioactively labeled rat IAPP (^{125}I-rIAPP) to BV-2 cells[38, 52]. ^{125}I-rIAPP exhibited appreciable and saturable binding at a tracer concentration of 100 pM, and binding was in the range of 3000-4000 cpm per 4 x 10^5 cells (data not shown). Of note, similar results were obtained when the human breast carcinoma cell line MCF-7 that expresses high-affinity IAPP receptors was applied (data not shown)[38, 52]. Importantly, ^{125}I-rIAPP binding was competed by both human IAPP and IAPP-GI, both known IAPP receptor agonists, in a dose-dependent manner, featuring similar binding isotherms ($IC_{50} \sim 1$ μM; **Figure 5D**)[38, 52]. This result suggested that BV-2 microglial cells express a functional IAPP receptor. We then tested binding of various concentrations of an aged mixture of Aβ40 with IAPP-GI (1/1) and of aged Aβ40 alone. The Aβ40/IAPP-GI mixture displaced ^{125}I-rIAPP from the microglial receptor with a similar binding isotherm as that seen for IAPP-GI alone, whereas aged Aβ40 alone did not exhibit significant binding to the IAPP receptor (**Figure 5E**). These findings indicated that Aβ/IAPP-GI hetero-oligomers are endocytosed by microglial cells via binding to an IAPP receptor. To confirm this observation[56] and further characterize the putative IAPP receptor, we performed immunoblot analysis of BV-2 lysates. AMY3 has previously been reported to be present in various areas of the human and rat brain and to mediate cytotoxic effects of both IAPP and Aβ[21, 23, 57]. We found that both AMY3 moieties, i.e. CTR and RAMP3, are expressed in the BV-2 microglial cells further underpinning the notion that Aβ/IAPP-GI and Aβ/IAPP hetero-oligomers are endocytosed via a receptor-mediated pathway involving IAPP-GI(IAPP)-mediated binding to AMY3 (**Figure 5F**). The data also insinuate that aggregated Aβ alone is taken up by a non-receptor-mediated slower route. In fact, this conclusion is in accord with the endocytosis inhibitor experiments (**Figure 5C**) and together suggests that Aβ/IAPP hetero-oligomers are endocytosed via a clathrin- and dynamin-dependent AMY3 receptor-mediated pathway[53, 58], whereas the Aβ alone-track may share the dynamin component with this pathway, but

likely does not involve any CME uptake components[59, 60]. This could also explain why the endocytosis inhibitors partially affected the uptake of Aβ40 alone at a similar relative rate, albeit at markedly lower overall levels and although this effect did not reach statistical significance.

Finally, we asked whether the observed inhibitory effect of IAPP-GI on caspase-1 activation caused by IAPP aggregates (*see* **Figure 1**), in analogy to the findings on Aβ/IAPP-GI hetero-oligomers, is also mediated by the uptake and efficient degradation of non-fibrillar IAPP-GI/IAPP hetero-oligomers [38]. To address this hypothesis, aged fibrillar IAPP versus IAPP-GI/IAPP (1/1) mixtures were incubated with primary BMDMs and lysosomal IAPP content was analyzed after 2 min, 2 h and 16 h of incubation by Western blot and bands quantified by densitometric analysis. Significant amounts of IAPP were found in lysosomes of cells incubated with fibrillar IAPP at the 2 and 16 h time intervals (**Figure 5G and H**), whereas the 2 min time point only showed faint IAPP bands, indicating the very early phase of uptake of the IAPP peptides (**Supplementary Figure S9**). Of note, markedly less IAPP was found in cells treated with the IAPP-GI/IAPP mixture. This difference was seen both at the early 2 h and the advanced 16 h time point of lysosomal exposure (**Figure 5G and H, Supplementary Figure S9**). These results supported the suggestion that nonfibrillar IAPP-GI/IAPP hetero-oligomers also become internalized by an AMY3 receptor-mediated pathway and are targeted to lysosomes, where they become more efficiently degraded than IAPP fibrils alone.

Conclusions. Taken together, our results show that the non-amyloidogenic IAPP analog IAPP-GI is able to prevent inflammatory responses of microglial cells and macrophages mediated by Aβ and IAPP aggregates. In addition, our results provide evidence that inhibition of Aβ-mediated microglial inflammation is mediated via a "dual-hit" mechanism (summarized in **Figure 6**). Accordingly, IAPP-GI appears to sequester Aβ or IAPP from their respective amyloidogenic pathway to funnel them into an IAPP receptor-mediated internalization pathway ("first hit"). IAPP receptor-mediated internalization is consistent with emerging evidence suggesting an important role for IAPP and the IAPP receptor in AD pathogenesis, although they do not exclude the possibility that additional uptake mechanisms may also exist for the Aβ/IAPP hetero-oligomers including binding to RAGE, CD36 or several of the other Aβ receptors and binding proteins, which are present in microglial cells[8, 24, 57, 61, 62].

We further conclude that hetero-complex formation between IAPP-GI and the amyloidogenic polypeptides results not only in their rapid endocytosis/internalization, but, in addition, serves to keep the amyloid component soluble and sensitive to degradation by the lysosomal enzyme armory ("second hit"). This in turn prevents lysosomal damage, lysosomal leakage, and attenuates the activation of NLRP3/caspase-1 and blocks IL-1β release that would otherwise amplify inflammation[1-3, 8-10, 17, 29]. Moreover, our results also suggest that the cross-interaction between non-fibrillar Aβ and IAPP species suppresses inflammatory cascades triggered by Aβ or IAPP assemblies in microglial cells by promoting lysosomal targeting via the IAPP receptor and proteolytic degradation of both polypeptides.

These results suggest that nonfibrillar Aβ/IAPP hetero-oligomers, if existent *in vivo*, may act to prevent Aβ- or IAPP-mediated inflammatory cascades in brain and pancreas[35]. While studies in animal models are now required to test the physiological relevance of the here suggested function of non-fibrillar Aβ/IAPP hetero-oligomers, emerging evidence supports the suggestion that functional disease-associated interactions between the two polypeptides exist *in vivo* as well[24, 30, 31, 63]. In fact, Aβ and IAPP, which are both present in blood and CSF at similar concentrations, have recently been found to colocalize in both cerebral and pancreatic amyloid deposits of AD and T2D patients while Aβ fibrils have been reported to cross-seed IAPP pancreatic amyloid deposition *in vivo*[30, 32, 36, 63-66].

Finally, our findings and recent results by others suggest that the use of "bifunctional" IAPP analogs that combine IAPP receptor agonist activity with the ability to bind Aβ40, Aβ42, and IAPP could become a promising approach to suppress inflammation in AD, T2D or both diseases[38, 67, 68]. Various anti-inflammatory compounds including NSAIDs, specific small molecule NLRP3 inflammasome inhibitors or compounds targeting IL-1β or its receptor are currently being evaluated in treating inflammatory diseases including AD and T2D[3, 10, 69-72]. While such compounds are potent and suppress a broad range of inflammatory processes including likely also beneficial ones, IAPP analogs might have the potential to even more specifically suppress Aβ or IAPP amyloidogenesis-mediated inflammatory cascades and might qualify for early targeted intervention approaches[1-3, 9, 10, 28, 69].

METHODS

Peptides and other compounds. Aβ40 was synthesized by Fmoc-solid phase peptide synthesis (SPPS), purified by RP-HPLC and treated as described[37, 73, 74]. Aβ40 stocks were freshly prepared in 1,1,3,3,3,3-hexafluoro-2-isopropanol (HFIP) (Aldrich) (4°C); their concentrations were determined by the bicinchoninic acid (BCA) assay (Pierce) as described[35, 37]. Synthetic Aβ42 and the pentapeptide LPFFD were from Bachem while glucagon was from Calbiochem. IAPP-GI, IAPP, and rIAPP were synthesized by Fmoc-solid phase synthesis methodology, oxidized and purified by RP-HPLC as described[38]. IAPP and IAPP-GI stocks were prepared in HFIP (4°C) and filtered over 0.2 μm filters (Millipore); their concentrations were determined by UV spectroscopy as described[38, 75]. N^{α}-amino-terminal fluorescein-labeled Aβ40, IAPP and IAPP-GI (Fluos-Aβ40, Fluos-IAPP and Fluos-IAPP-GI) and tetra-methylrhodamin (TAMRA)-labeled Aβ40 (Rhodamin-Aβ40) were synthesized by SPPS purified and their HFIP stocks made and handled as described[35, 37, 38]. Concentrations of fluorescently labeled peptides were determined by UV spectroscopy as described[35, 37]. All synthetic peptides were characterized by matrix-assisted laser desorption ionization mass spectroscopy (MALDI-MS). Epigallocatechin gallate (EGCG) was from Aldrich.

Cell culture. The mouse microglial cell line BV-2 as well as the immortalized *Nlrp3*-knock out and wildtype (WT) peritoneal exudate mouse macrophages were cultured in DMEM (Gibco) supplemented with 10% (vol/vol) heat-inactivated fetal calf serum (FCS), 4.5 g/L D-glucose, 2 mM L-glutamine, 1 mM sodium pyruvate (all from Gibco), and 0.1 mg/ml penicillin/streptomycin (Invitrogen). Murine bone marrow-derived macrophages (BMDMs) were cultured in RPMI 1640 medium supplemented with 10% (vol/vol) heat-inactivated FCS, 4.5 g/L D-glucose, 2 mM L-glutamine/pyruvate (Gibco), and 0.1 mg/mL penicillin/streptomycin (Invitrogen) plus 25 ng/mL monocyte-colony stimulating factor (M-CSF) (R&D). Cells were incubated in a humidified atmosphere with 5% CO_2 at 37°C.

Isolation and differentiation of bone marrow-derived macrophages. Bone marrow-derived macrophages (BMDM) were generated from 8 week-old female WT C57BL/6 mice essentially as described recently[76]. Isolated bone marrow cell suspensions were differentiated and grown by adding 25 ng/mL M-

CSF and incubation in a humidified incubator with 5% CO2 at 37°C for 7 days. Every 2-3 days, differentiating cells were washed with RPMI medium and supplied with fresh medium plus 25 ng/mL M-CSF. Under these conditions, the bone marrow monocyte/macrophage progenitors proliferated and differentiated into a homogenous population of mature BMDMs. The efficiency of the differentiation was assessed by fluorescence-activated cell sorting (FACS) analysis detecting F4/80 surface antigen expression as described[76].

Determination of fibrillogenesis by the ThT binding assay. Previously established assay protocols were essentially applied[35, 38]. Briefly, peptides were dissolved in HFIP and then dried-off with nitrogen purging. The residual peptide was redissolved in thioflavin T (ThT) assay buffer (50 mM sodium phosphate buffer, pH 7.4, 100 mM NaCl, containing 1% HFIP for Aβ-related assays or 0.5% HFIP for IAPP-related incubations) to a concentration of 100 μM. Solutions were incubated (unstirred) at room temperature for 1-4 days and amyloidogenesis was determined by the ThT binding assay. ThT binding was measured in aliquots of the incubations of IAPP, Aβ40 and IAPP-GI alone and Aβ40 or IAPP mixtures with IAPP-GI (1/1) (parallel incubations were always performed) by mixing with a ThT solution (5 μM ThT in 100 mM glycine/NaOH buffer, pH 8.5) and then immediately measuring fluorescence emission at 486 nm after excitation at 450 nm using a 1420 Multilabel Counter Victor (PerkinElmer Life Sciences) as described[35, 38].

Caspase-1 activation assay.

In BV-2 microglial cells (with or without LPS stimulation). *With LPS stimulation:* To measure caspase-1 activation, BV-2 microglial cells at a density of 0.55 x 10^6 cells/plate (0.36 x 10^4/mL) were seeded on 3.5 cm poly-L-ornithine-coated tissue culture dishes (Sarstedt) and grown in DMEM medium (Gibco) supplemented with 10% (vol/vol) FCS at 37°C (under 5% CO_2) for 24 h. Cells were starved in serum-free DMEM for at least 4 h before stimulation with 100 ng/mL lipopolysaccharide (LPS; serotype O111:B4; Sigma-Aldrich, Steinheim, Germany). After 4 h exposure to LPS, solutions of 4 day-aged Aβ40 (100 μM) or Aβ40+IAPP-GI (1/1) in 50 mM sodium phosphate buffer, pH 7.4, containing 100 mM NaCl plus 1% HFIP, were diluted with cell culture medium and added to the cells to a final peptide

concentration of 10 μM. The 1/1 ratio of Aβ and IAPP-GI had previously been demonstrated to convey complete inhibition of Aβ fibrillogenesis. As a positive control, ATP (Aldrich) was added to some incubations at a final concentration of 1 mM and cells incubated for 30 min at 37°C. After 30 min incubation with ATP, medium was replaced with FCS-free medium and samples (treated or untreated) incubated overnight at 37°C. Medium was removed, cells were rinsed twice with cold PBS (Aldrich), detached and incubated with FLICA substrate (Immunochemistry Technologies, United States) for 1 h at 37°C (5% CO_2) according to the manufacturer's instructions. Cells were washed and fluorescence intensity was measured at 535 nm following excitation at 485 nm using the 1420 Multilabel Counter Victor. *Without LPS stimulation:* The experimental procedure was as above except that after 4 h of starvation in DMEM medium without FCS, peptide solutions were added to the cells without prior LPS stimulation. Aβ42 incubations were the same as for Aβ40 (i.e. 100 μM; Aβ42/IAPP-GI at 1/1).

In immortalized peritoneal mouse macrophages (PMs). Wildtype (WT) or *Nlrp3*$^{-/-}$ macrophages were seeded in 3.5 cm-tissue culture dishes a density of 0.6 x 10^6 cells/plate (equal to 0.4 x 10^6/mL) (Sarstedt) and grown in DMEM supplemented with 10% (v/v) FCS at 37°C (5% CO_2) for 24 h. Cells were starved in serum-free DMEM for at least 4 h before addition of incubations of aged peptides (100 μM in 50 mM sodium phosphate buffer, pH 7.4, containing 100 mM NaCl and 0.5% HFIP) following their dilution with cell culture medium (final peptide concentration on cells: 5 μM). After 16 h incubation, medium was removed, cells were rinsed twice with cold PBS and detached from plates. Caspase-1 activity using FLICA substrate was determined as above.

In bone marrow-derived macrophages (BMDMs). After BMDMs were isolated and differentiated for 7 days (see above), cells at a density of 1 x 10^6 cells/mL were seeded in 3.5 cm tissue culture dishes and grown for 3 days at 37°C (5% CO_2) in RPMI 1640 medium supplemented with FCS (10%) and 25 ng/mL M-CSF. Cells were starved in serum-free RPMI 1640 medium for 24 h before addition of solutions of the pre-incubated peptides as above at a 1/1 ratio. Caspase-1 activity using FLICA substrate was determined as above.

Detection of active caspase-1 by measuring subunit p10. Cleaved caspase-1 fragment p10 was measured by Western blot essentially following an established procedure[77]. The caspase-1 p10 (M-20) antibody sc-514 (Santa Cruz Biotechnology) was used to develop the Western blot membrane.

Assessment of cell damage via the MTT reduction assay. The 3-[4,5 dimethylthiazol-2-yl]-2,5-diphenyltetrazolium bromide (MTT) reduction assay was performed as previously described[35, 38].

Cathepsin B activity assay. Cathepsin B assays were performed in lysates of BV-2 microglial cells. Cells were seeded and grown as above and starved in serum-free DMEM at least 4 h. Aliquots of 4 day-aged solutions of Aβ40 (100 μM), Aβ40+IAPP-GI (100 μM each) in 50 mM sodium phosphate buffer, pH 7.4, containing 100 mM NaCl and 1% HFIP were diluted with cell medium and added to the cells at a final peptide concentration of 10 μM. Following overnight incubation and washing (twice), cells were detached and mixed with Magic Red substrate (Immunochemistry Technologies, United States) [78]. After incubation for 1 h at 37°C (5% CO_2), cells were washed, resuspended in PBS and fluorescence at 590 nm was measured following excitation at 485 nm using the 1420 Multilabel Counter Victor [78].

IL-1β enzyme-linked immunosorbent assay (ELISA). BV-2 microglial cells were sub-cultured at a density of 0.55 x 10^6 cells/plate (0.36 x 10^6/ml) in 3.5 cm poly-L-ornithine-coated tissue culture dishes for 24 h (Sarstedt). Thereafter, medium was replaced with serum-free DMEM for at least 4 h before applying 100 ng/ml LPS. After 4 h stimulation with LPS, aged peptide incubations (for preparation see above) were added to the cells at a final concentration of 10 μM. ATP (final concentration 1 mM) was used as a positive control. After 30 min of incubation with ATP, medium was replaced with FCS-free DMEM. Treated and untreated cells were incubated for 16 h at 37°C (5% CO_2) and supernatants were collected and assayed for IL-1β content using an IL-1β ELISA kit (Peprotech, United States) according to the manufacturer´s instructions.

Western blot (WB) analysis. Western blot was used for semi-quantification of peptides in cell supernatants or lysosomal compartments and to identify IAPP receptor components in BV-2 cells following previously established protocols[76, 79]. Briefly, for the quantification of Aβ in cell supernatants, BV-2 microglial cells were plated on poly-ornithine-coated 96-well plates (Nunc) at a density of 0.15 x 10^5 per well (i.e. per 300 μL) and incubated overnight at 37°C (5% CO_2). Thereafter, cells were starved

for 4 h in serum-free DMEM. 4 day-aged solutions of fibrillar Aβ40 (100 μM) or mixtures of Aβ40 with IAPP-GI (100 μM each) in 50 mM sodium phosphate buffer, pH 7.4, containing 100 mM NaCl and 1% HFIP were diluted with cell culture medium and added to the cells at a final peptide concentration of 10 μM. Incubations were performed up to 16 h. At the indicated time points supernatants were collected, lyophilized and dissolved in reducing NuPAGE sample loading buffer (Invitrogen) and boiled for 5 min. Samples were subjected to NuPAGE electrophoresis in 4-12% Bis-Tris gels with MES running (Invitrogen) and blotted onto nitrocellulose membrane. Amyloid peptides were revealed by Western blotting using a polyclonal rabbit antibody anti-Aβ(1-40) (Sigma) in combination with HRP-coupled secondary antibody (Amersham) and the Super Signal Duration ECL staining solution (Pierce). For Western blot analysis of lysosomal fractions, see under "Peptide uptake and degradation assays".

To determine whether the IAPP receptor is expressed in BV-2 microglial cells, 0.25 x 10^6 cells were lysed with reducing NuPAGE sample loading buffer and boiled for 5 min, followed by sonification for 15 min at 4°C. Samples were subjected to NuPAGE and blotted. Receptor components were revealed by incubation with polyclonal rabbit anti-CTR antibody (CTR, Calcitonin receptor) and by polyclonal rabbit anti-RAMP3 antibody (Abcam) together with HRP-coupled secondary antibody (Amersham) and the Super Signal Duration ECL staining solution (Pierce).

Peptide uptake, degradation, and lysosomal integrity assays. BV-2 microglial cells were seeded at a density of 0.35 x 10^6 cells/plate (0.125 x 10^6/ml) on sterile poly-ornithine pre-coated glass coverslips (Thermo Scientific) and grown at 37°C (5% CO_2) for 24 h. Thereafter, aliquots of solutions of Fluos-IAPP, Fluos-IAPP-GI, Fluos-Aβ, Rhodamin-Aβ, and Fluos-Aβ+IAPP-GI (1/1) or Rhodamin-Aβ+Fluos-IAPP-GI (1/1) in 50 mM sodium phosphate, pH 7.4, containing 100 mM NaCl (peptide concentration: 2 μM) were diluted with cell medium and added to the cells at a final concentration of 200 nM. Cells were incubated with peptides for 16 h (37°C, protected from light). Coverslips were then mounted on an Axiovert 100 M confocal laser-scanning microscope (Zeiss, Jena, Germany) and medium was replaced with 1 ml phenol red-free DMEM medium (Gibco). To stain lysosomes, the acidophilic lysotropic dye Lysotracker Red DND-99 (Invitrogen) was added to the cells at a concentration of 40 nM and incubated 10-15 min with the cells at room temperature.

To analyze amyloid peptide uptake and degradation biochemically, pre-cultivated BV-2 microglia cells or BMDMs were seeded on polyornithine-coated plates, starved in serum-free medium before stimulation with aged peptide solutions. Cells were incubated with peptide solutions as indicated (10 µM for BV-2 and 2 µM for BMDMs) for 0, 2, or 16 h at 37°C. Washed and pelleted cells were homogenized using a Dounce homogenizer and lysosomes enriched by differential centrifugation. For uptake assays, cells were additionally washed with cold PBS (three times) and once with glycine buffer (pH 2.8) before detaching, pelleting, and homogenization on ice to remove non-specifically adhered peptides.

To prepare lysosomal extracts, lysosomes were lysed by 6 cycles of freeze and thaw with 15 sec vortexing between each cycle. The lysed lysosomes were centrifuged at 10.000 x g, 10 min, 4°C to separate lysosomal debris from extracts. Lysosomal extracts were added to 4 days aged solutions of Aβ40 (100 µM) or Aβ40+IAPP-GI (1/1; 100 µM) (in 50 mM sodium phosphate buffer, pH 7.4, containing 100 mM NaCl plus 1% HFIP. Samples were diluted to a final peptide concentration of 10 µM with incubation buffer and the pH value was adjusted to a value of 5.0 to adapt to lysosomal pH conditions. Following overnight incubation, solutions were subjected to NuPAGE (4-12% Bis-Tris gels with MES running buffer) and WB with a polyclonal rabbit antibody anti-Aβ(1-40) as above or to MALDI-MSLysosomal integrity was probed by measuring cathepsin B content by Western blot using a mouse monoclonal antibody to cathepsin B (Abcam). LAMP1, a lysosomal transmembrane protein, was probed by incubating the membrane with a mouse monoclonal anti-LAMP-1 antibody (Abcam).

To study peptide degradation by lysosomal extracts, lysosomes were lysed by 6 cycles of freeze and thaw with 15 sec vortexing between each cycle. Lysed lysosomes were cleared from debris and added to 4 day-aged solutions of Aβ40 (100 µM) or Aβ40+IAPP-GI (1/1; 100 µM) (final peptide concentration 10 µM, pH 5.0) and incubated overnight.

For the study of peptide degradation by purified cathepsin B, peptide incubations were prepared as above. Purified cathepsin B from bovine spleen (Aldrich) was dissolved and activated in 20 mM sodium acetate buffer (pH 5) containing 1 mM EDTA and 2 mM DTT and added to the preincubated peptides. Samples were then diluted with the sodium acetate buffer to a final peptide concentration of 10 µM, the

pH value was adjusted again to 5 and incubations were allowed to procede overnight. Digests were subjected to NuPAGE electrophoresis as above.

IAPP receptor binding assay. The receptor binding studies were performed in BV-2 cells following a modification of an established procedure[79]. Briefly, BV-2 microglial cells were plated on polyornithine-coated plates and incubated in low-serum DMEM on ice for 20-30 min. Peptides were added at indicated final concentrations followed by addition of ^{125}I-rIAPP (100 pM) and cells incubated on ice for 1.5 h, washed, and lysed. Bound ^{125}I-rIAPP was quantified using liquid scintillation counting.

Endocytosis inhibition assay. BV-2 microglial cells were plated on polyornithin-coated plates (Nunc) at a density of 0.015 x 10^6 per well (or per 300 μL) and incubated overnight at 37°C. Cells were starved for 4 h in serum-free DMEM before adding endocytosis inhibitors. Cells were then exposed to 50 μM monodansylcadaverine (MDC) (Sigma) and 80 μM dynasore (Sigma) and incubated for 30 min at 37°C. Aliquots of 4 day-aged solutions of Aβ40 alone (100 μM) or Aβ40+IAPP-GI (1:1) (in 50 mM sodium phosphate buffer, pH 7.4, with 100 mM NaCl and 0.5% HFIP) were diluted with cell culture medium and added to the cells to a final concentration of 10 μM. After incubating with peptides for 2, 30 and 60 min, cells were washed with glycine buffer (pH 2.8), mixed with reducing NuPAGE sample loading buffer, boiled for 5 min and subjected to NuPAGE electrophoresis and WB as above.

Statistical analysis. Numerical data were expressed as mean±SEM. Student's t-tests (two-sided, unpaired) as well as one-way ANOVA Bonferroni post-test were performed.

AUTHOR INFORMATION

Author Contributions

M.A. performed the amyloid-triggered inflammasome activation experiments and inhibition studies with IAPP-GI and IAPP in microglial cells and macrophages. She also performed parts of the aggregation and receptor internalization and binding experiments. She participated in the experimental design, data analysis and discussion. M.T.N. performed parts of the aggregation experiments and receptor internalization studies. She participated in preparing the amyloid peptides and their analogs, and in data analysis and discussion. E.A. synthesized and prepared the IAPP, IAPP-GI, and Aβ peptides. M.K. and C.B. provided the microglial cells and participated in experimental design and discussions. E.L. provided the Nlrp3-KO cell line and participated in discussions. J.B. and A.K. supervised the entire project, designed the experiments, analyzed data, and wrote the manuscript.

Acknowledgements

We thank Dr. Hongqi Lue for advice with the biochemical and microscopic experiments, and Andrea Stutz for technical support with the *Nlrp3*-KO macrophages. We acknowledge help from Markus Brandhofer with the caspase 1-p10 fragmentation analysis and from Chunfang Zan with blot quantifications. Further, this work was supported by the Immunohistochemistry and Confocal Microscopy Unit, a core facility of the Interdisciplinary Center for Clinical Research (IZKF) Aachen within the Faculty of Medicine at RWTH Aachen University.

Funding

This study was supported by funds from Deutsche Forschungsgemeinschaft (DFG) grant IRTG1508 to J.B. and M.A., DFG grant SFB1035-B06 to A.K., and DFG grant SFB-TRR57 to E.L. J.B. was also funded by DFG under Germany's Excellence Strategy within the framework of the Munich Cluster for Systems Neurology (EXC 1010 and 2145 SyNergy – ID 390857198).

Notes

A.K., J.B., and E.A. are co-inventors on a patent describing amyloidogenesis-blocking IAPP derivatives.

The other authors declare no competing financial interests.

ASSOCIATED CONTENT

Supporting information

The Supporting Information is available free of charge on the ACS Publications website at DOI: xxxx/acschemneuro.

It contains: Supplementary Figures S1 – S9.

REFERENCES

[1] Wyss-Coray, T. (2006) Inflammation in Alzheimer disease: driving force, bystander or beneficial response?, *Nat Med 12*, 1005-1015.

[2] Heneka, M. T., Kummer, M. P., and Latz, E. (2014) Innate immune activation in neurodegenerative disease, *Nat Rev Immunol 14*, 463-477.

[3] Meraz-Rios, M. A., Toral-Rios, D., Franco-Bocanegra, D., Villeda-Hernandez, J., and Campos-Pena, V. (2013) Inflammatory process in Alzheimer's Disease, *Front Integr Neurosci 7*, 59.

[4] Labzin, L. I., Heneka, M. T., and Latz, E. (2018) Innate immunity and neurodegeneration, *Annu Rev Med 69*, 437-449.

[5] Heppner, F. L., Ransohoff, R. M., and Becher, B. (2015) Immune attack: the role of inflammation in Alzheimer disease, *Nat Rev Neurosci 16*, 358-372.

[6] Ransohoff, R. M. (2016) How neuroinflammation contributes to neurodegeneration, *Science 353*, 777-783.

[7] Salter, M. W., and Stevens, B. (2017) Microglia emerge as central players in brain disease, *Nat Med 23*, 1018-1027.

[8] Block, M. L., Zecca, L., and Hong, J. S. (2007) Microglia-mediated neurotoxicity: uncovering the molecular mechanisms, *Nat Rev Neurosci 8*, 57-69.

[9] Prokop, S., Miller, K. R., and Heppner, F. L. (2013) Microglia actions in Alzheimer's disease, *Acta Neuropathol 126*, 461-477.

[10] McGeer, P. L., and McGeer, E. G. (2013) The amyloid cascade-inflammatory hypothesis of Alzheimer disease: implications for therapy, *Acta Neuropathol 126*, 479-497.

[11] Cohen, S. I. A., Cukalevski, R., Michaels, T. C. T., Saric, A., Tornquist, M., Vendruscolo, M., Dobson, C. M., Buell, A. K., Knowles, T. P. J., and Linse, S. (2018) Distinct thermodynamic signatures of oligomer generation in the aggregation of the amyloid-beta peptide, *Nat Chem 10*, 523-531.

[12] Simard, A. R., Soulet, D., Gowing, G., Julien, J. P., and Rivest, S. (2006) Bone marrow-derived microglia play a critical role in restricting senile plaque formation in Alzheimer's disease, *Neuron 49*, 489-502.

[13] Griffin, W. S., Stanley, L. C., Ling, C., White, L., MacLeod, V., Perrot, L. J., White, C. L., 3rd, and Araoz, C. (1989) Brain interleukin 1 and S-100 immunoreactivity are elevated in Down syndrome and Alzheimer disease, *Proc Natl Acad Sci U S A 86*, 7611-7615.

[14] Blum-Degen, D., Muller, T., Kuhn, W., Gerlach, M., Przuntek, H., and Riederer, P. (1995) Interleukin-1 beta and interleukin-6 are elevated in the cerebrospinal fluid of Alzheimer's and de novo Parkinson's disease patients, *Neurosci Lett 202*, 17-20.

[15] Heneka, M. T., Kummer, M. P., Stutz, A., Delekate, A., Schwartz, S., Vieira-Saecker, A., Griep, A., Axt, D., Remus, A., Tzeng, T. C., Gelpi, E., Halle, A., Korte, M., Latz, E., and Golenbock, D. T. (2013) NLRP3 is activated in Alzheimer's disease and contributes to pathology in APP/PS1 mice, *Nature 493*, 674-678.

[16] Latz, E., Xiao, T. S., and Stutz, A. (2013) Activation and regulation of the inflammasomes, *Nat Rev Immunol 13*, 397-411.

[17] Halle, A., Hornung, V., Petzold, G. C., Stewart, C. R., Monks, B. G., Reinheckel, T., Fitzgerald, K. A., Latz, E., Moore, K. J., and Golenbock, D. T. (2008) The NALP3 inflammasome is involved in the innate immune response to amyloid-beta, *Nat Immunol 9*, 857-865.

[18] Jin, S., Kedia, N., Illes-Toth, E., Haralampiev, I., Prisner, S., Herrmann, A., Wanker, E. E., and Bieschke, J. (2016) Amyloid-beta(1-42) Aggregation Initiates Its Cellular Uptake and Cytotoxicity, *J Biol Chem 291*, 19590-19606.

[19] Heneka, M. T., McManus, R. M., and Latz, E. (2018) Inflammasome signalling in brain function and neurodegenerative disease, *Nat Rev Neurosci 19*, 610-621.

[20] Venegas, C., Kumar, S., Franklin, B. S., Dierkes, T., Brinkschulte, R., Tejera, D., Vieira-Saecker, A., Schwartz, S., Santarelli, F., Kummer, M. P., Griep, A., Gelpi, E., Beilharz, M., Riedel, D., Golenbock, D. T., Geyer, M., Walter, J., Latz, E., and Heneka, M. T. (2017) Microglia-derived ASC specks cross-seed amyloid-beta in Alzheimer's disease, *Nature 552*, 355-361.

[21] Westermark, P., Andersson, A., and Westermark, G. T. (2011) Islet amyloid polypeptide, islet amyloid, and diabetes mellitus, *Physiol Rev 91*, 795-826.

[22] Westermark, G. T., and Westermark, P. (2013) Islet amyloid polypeptide and diabetes, *Curr Protein Pept Sci 14*, 330-337.

[23] Morfis, M., Tilakaratne, N., Furness, S. G., Christopoulos, G., Werry, T. D., Christopoulos, A., and Sexton, P. M. (2008) Receptor activity-modifying proteins differentially modulate the G protein-coupling efficiency of amylin receptors, *Endocrinology 149*, 5423-5431.

[24] Roth, J. D., Maier, H., Chen, S., and Roland, B. L. (2009) Implications of Amylin Receptor Agonism: Integrated neurohormonal mechanisms and therapeutic applications, *Arch Neurol 66*, 306-310.

[25] Westwell-Roper, C. Y., Ehses, J. A., and Verchere, C. B. (2014) Resident macrophages mediate islet amyloid polypeptide-induced islet IL-1beta production and beta-cell dysfunction, *Diabetes 63*, 1698-1711.

[26] Badman, M. K., Pryce, R. A., Charge, S. B., Morris, J. F., and Clark, A. (1998) Fibrillar islet amyloid polypeptide (amylin) is internalised by macrophages but resists proteolytic degradation, *Cell Tissue Res 291*, 285-294.

[27] Masters, S. L., Dunne, A., Subramanian, S. L., Hull, R. L., Tannahill, G. M., Sharp, F. A., Becker, C., Franchi, L., Yoshihara, E., Chen, Z., Mullooly, N., Mielke, L. A., Harris, J., Coll, R. C., Mills, K. H., Mok, K. H., Newsholme, P., Nunez, G., Yodoi, J., Kahn, S. E., Lavelle, E. C., and O'Neill, L. A. (2010) Activation of the NLRP3 inflammasome by islet amyloid polypeptide provides a mechanism for enhanced IL-1beta in type 2 diabetes, *Nat Immunol 11*, 897-904.

[28] Mandrup-Poulsen, T. (2010) IAPP boosts islet macrophage IL-1 in type 2 diabetes, *Nat Immunol 11*, 881-883.

[29] Masters, S. L., and O'Neill, L. A. (2011) Disease-associated amyloid and misfolded protein aggregates activate the inflammasome, *Trends Mol Med 17*, 276-282.

[30] Oskarsson, M. E., Paulsson, J. F., Schultz, S. W., Ingelsson, M., Westermark, P., and Westermark, G. T. (2015) In Vivo Seeding and Cross-Seeding of Localized Amyloidosis: A Molecular Link between Type 2 Diabetes and Alzheimer Disease, *Am J Pathol 185*, 834-846.

[31] Sun, M.-K., and Alkon, D. L. (2006) Links between Alzheimer's disease and Diabetes, *Drugs Today 42*, 481-489.

[32] Miklossy, J., Qing, H., Radenovic, A., Kis, A., Vileno, B., Laszlo, F., Miller, L., Martins, R. N., Waeber, G., Mooser, V., Bosman, F., Khalili, K., Darbinian, N., and McGeer, P. L. (2010) Beta

amyloid and hyperphosphorylated tau deposits in the pancreas in type 2 diabetes, *Neurobiol Aging 31*, 1503-1515.

[33] Akter, K., Lanza, E. A., Martin, S. A., Myronyuk, N., Rua, M., and Raffa, R. B. (2011) Diabetes mellitus and Alzheimer's disease: shared pathology and treatment?, *Br J Clin Pharmacol 71*, 365-376.

[34] Zhu, H., Wang, X., Wallack, M., Li, H., Carreras, I., Dedeoglu, A., Hur, J. Y., Zheng, H., Li, H., Fine, R., Mwamburi, M., Sun, X., Kowall, N., Stern, R. A., and Qiu, W. Q. (2015) Intraperitoneal injection of the pancreatic peptide amylin potently reduces behavioral impairment and brain amyloid pathology in murine models of Alzheimer's disease, *Mol Psych 20*, 252-262.

[35] Yan, L. M., Velkova, A., Tatarek-Nossol, M., Andreetto, E., and Kapurniotu, A. (2007) IAPP mimic blocks Abeta cytotoxic self-assembly: cross-suppression of amyloid toxicity of Abeta and IAPP suggests a molecular link between Alzheimer's disease and type II diabetes, *Angew Chem Int Ed Engl 46*, 1246-1252.

[36] O'Nuallain, B., Williams, A. D., Westermark, P., and Wetzel, R. (2004) Seeding specificity in amyloid growth induced by heterologous fibrils, *J Biol Chem 279*, 17490-17499.

[37] Andreetto, E., Yan, L. M., Tatarek-Nossol, M., Velkova, A., Frank, R., and Kapurniotu, A. (2010) Identification of hot regions of the Abeta-IAPP interaction interface as high-affinity binding sites in both cross- and self-association, *Angew Chem Int Ed Engl 49*, 3081-3085.

[38] Yan, L. M., Tatarek-Nossol, M., Velkova, A., Kazantzis, A., and Kapurniotu, A. (2006) Design of a mimic of nonamyloidogenic and bioactive human islet amyloid polypeptide (IAPP) as nanomolar affinity inhibitor of IAPP cytotoxic fibrillogenesis, *Proc Natl Acad Sci U S A 103*, 2046-2051.

[39] Bakou, M., Hille, K., Kracklauer, M., Spanopoulou, A., Frost, C. V., Malideli, E., Yan, L. M., Caporale, A., Zacharias, M., and Kapurniotu, A. (2017) Key aromatic/hydrophobic amino acids controlling a cross-amyloid peptide interaction versus amyloid self-assembly, *J Biol Chem 292*, 14587-14602.

[40] Spanopoulou, A., Heidrich, L., Chen, H. R., Frost, C., Hrle, D., Malideli, E., Hille, K., Grammatikopoulos, A., Bernhagen, J., Zacharias, M., Rammes, G., and Kapurniotu, A. (2018) Designed macrocyclic peptides as nanomolar amyloid inhibitors based on minimal recognition elements, *Angew Chem Int Ed Engl 57*, 14503-14508.

[41] Habib, P., Dreymueller, D., Ludwig, A., Beyer, C., and Dang, J. (2013) Sex steroid hormone-mediated functional regulation of microglia-like BV-2 cells during hypoxia, *J Steroid Biochem Mol Biol 138*, 195-205.

[42] Habib, P., Slowik, A., Zendedel, A., Johann, S., Dang, J., and Beyer, C. (2014) Regulation of hypoxia-induced inflammatory responses and M1-M2 phenotype switch of primary rat microglia by sex steroids, *J Mol Neurosci 52*, 277-285.

[43] Henn, A., Lund, S., Hedtjarn, M., Schrattenholz, A., Porzgen, P., and Leist, M. (2009) The suitability of BV2 cells as alternative model system for primary microglia cultures or for animal experiments examining brain inflammation, *Altex 26*, 83-94.

[44] Fassbender, K., Walter, S., Kuhl, S., Landmann, R., Ishii, K., Bertsch, T., Stalder, A. K., Muehlhauser, F., Liu, Y., Ulmer, A. J., Rivest, S., Lentschat, A., Gulbins, E., Jucker, M., Staufenbiel, M., Brechtel, K., Walter, J., Multhaup, G., Penke, B., Adachi, Y., Hartmann, T., and Beyreuther, K. (2004) The LPS receptor (CD14) links innate immunity with Alzheimer's disease, *FASEB J 18*, 203-205.

[45] Yates, S. L., Burgess, L. H., Kocsis-Angle, J., Antal, J. M., Dority, M. D., Embury, P. B., Piotrkowski, A. M., and Brunden, K. R. (2000) Amyloid β and amylin fibrils induce increases in proinflammatory cytokine and chemokine production by THP-1 cells and murine microglia, *J Neurochem 74*, 1017-1025.

[46] Hu, X., Crick, S. L., Bu, G., Frieden, C., Pappu, R. V., and Lee, J. M. (2009) Amyloid seeds formed by cellular uptake, concentration, and aggregation of the amyloid-beta peptide, *Proc Natl Acad Sci U S A 106*, 20324-20329.

[47] Mueller-Steiner, S., Zhou, Y., Arai, H., Roberson, E. D., Sun, B., Chen, J., Wang, X., Yu, G., Esposito, L., Mucke, L., and Gan, L. (2006) Antiamyloidogenic and neuroprotective functions of cathepsin B: implications for Alzheimer's disease, *Neuron 51*, 703-714.

[48] Chung, H., Brazil, M. I., Soe, T. T., and Maxfield, F. R. (1999) Uptake, degradation, and release of fibrillar and soluble forms of Alzheimer's amyloid beta-peptide by microglial cells, *J Biol Chem 274*, 32301-32308.

[49] Soto, C., Sigurdsson, E. M., Morelli, L., Kumar, R. A., Castano, E. M., and Frangione, B. (1998) β-sheet breaker peptides inhibit fibrillogenesis in rat brain model of amyloidosis: Implications for Alzheimer's therapy, *Nat Med 4*, 822-826.

[50] Ehrnhoefer, D. E., Bieschke, J., Boeddrich, A., Herbst, M., Masino, L., Lurz, R., Engemann, S., Pastore, A., and Wanker, E. E. (2008) EGCG redirects amyloidogenic polypeptides into unstructured, off-pathway oligomers, *Nat Struct Mol Biol 15*, 558-566.

[51] Bailey, R. J., Walker, C. S., Ferner, A. H., Loomes, K. M., Prijic, G., Halim, A., Whiting, L., Phillips, A. R., and Hay, D. L. (2012) Pharmacological characterization of rat amylin receptors: implications for the identification of amylin receptor subtypes, *Br J Pharmacol 166*, 151-167.

[52] Zimmermann, U., Fluehmann, B., Born, W., Fischer, J. A., and Muff, R. (1997) Coexistence of novel amylin-binding sites with calcitonin receptors in human breast carcinoma MCF-7 cells, *J Endocrinol 155*, 423-431.

[53] Guo, S., Zhang, X., Zheng, M., Zhang, X., Min, C., Wang, Z., Cheon, S. H., Oak, M. H., Nah, S. Y., and Kim, K. M. (2015) Selectivity of commonly used inhibitors of clathrin-mediated and caveolae-dependent endocytosis of G protein-coupled receptors, *Biochim Biophys Acta 1848*, 2101-2110.

[54] Mayor, S., and Pagano, R. E. (2007) Pathways of clathrin-independent endocytosis, *Nat Rev Mol Cell Biol 8*, 603-612.

[55] Kettenmann, H., Hanisch, U. K., Noda, M., and Verkhratsky, A. (2011) Physiology of microglia, *Physiol Rev 91*, 461-553.

[56] Fu, W., Vukojevic, V., Patel, A., Soudy, R., MacTavish, D., Westaway, D., Kaur, K., Goncharuk, V., and Jhamandas, J. (2017) Role of microglial amylin receptors in mediating beta amyloid (Abeta)-induced inflammation, *J Neuroinflamm 14*, 199.

[57] Fu, W., and Jhamandas, J. H. (2013) Role of amylin and its receptors in neurodegeneration, *Curr Protein Pept Sci 14*, 338-345.

[58] Hilairet, S., Foord, S. M., Marshall, F. H., and Bouvier, M. (2001) Protein-protein interaction and not glycosylation determines the binding selectivity of heterodimers between the calcitonin receptor-like receptor and the receptor activity-modifying proteins, *J Biol Chem 276*, 29575-29581.

[59] Omtri, R. S., Davidson, M. W., Arumugam, B., Poduslo, J. F., and Kandimalla, K. K. (2012) Differences in the cellular uptake and intracellular itineraries of amyloid beta proteins 40 and 42: ramifications for the Alzheimer's drug discovery, *Mol Pharm 9*, 1887-1897.

[60] Wesen, E., Jeffries, G. D. M., Matson Dzebo, M., and Esbjorner, E. K. (2017) Endocytic uptake of monomeric amyloid-beta peptides is clathrin- and dynamin-independent and results in selective accumulation of Abeta(1-42) compared to Abeta(1-40), *Sci Rep 7*, 2021.

[61] Yu, Y., and Ye, R. D. (2015) Microglial Abeta receptors in Alzheimer's disease, *Cell Mol Neurobiol 35*, 71-83.

[62] Koenigsknecht, J., and Landreth, G. (2004) Microglial phagocytosis of fibrillar beta-amyloid through a beta1 integrin-dependent mechanism, *J Neurosci 24*, 9838-9846.

[63] Jackson, K., Barisone, G. A., Diaz, E., Jin, L. W., DeCarli, C., and Despa, F. (2013) Amylin deposition in the brain: A second amyloid in Alzheimer disease?, *Ann Neurol 74*, 517-526.

[64] Banks, W. A., Kastin, A. J., Maness, L. M., Huang, W., and Jaspan, J. B. (1995) Permeability of the blood-brain barrier to amylin, *Life Sci 57*, 1993-2001.

[65] Ida, N., Hartmann, T., Pantel, J., Schröder, J., Zerfass, R., Förstl, H., Sandbrink, R., Masters, C. L., and Beyreuther, K. (1996) Analysis of heterogeneous βA4 peptides in human cerebrospinal fluid and blood by a newly developed sensitive western blot assay, *J Biol Chem 271*, 22908-22914.

[66] Sanke, T., Hanabusa, T., Nakano, Y., Oki, C., Okai, K., Nishimura, S., Kondo, M., and Nanjo, K. (1991) Plasma islet amyloid polypeptide (Amylin) levels and their responses to oral glucose in type 2 (non-insulin-dependent) diabetic patients, *Diabetologia 34*, 129-132.

[67] Yan, L. M., Velkova, A., Tatarek-Nossol, M., Rammes, G., Sibaev, A., Andreetto, E., Kracklauer, M., Bakou, M., Malideli, E., Goke, B., Schirra, J., Storr, M., and Kapurniotu, A. (2013) Selectively N-methylated soluble IAPP mimics as potent IAPP receptor agonists and nanomolar

inhibitors of cytotoxic self-assembly of both IAPP and Abeta40, *Angew Chem Int Ed Engl 52*, 10378-10383.

[68] Adler, B. L., Yarchoan, M., Hwang, H. M., Louneva, N., Blair, J. A., Palm, R., Smith, M. A., Lee, H. G., Arnold, S. E., and Casadesus, G. (2014) Neuroprotective effects of the amylin analogue pramlintide on Alzheimer's disease pathogenesis and cognition, *Neurobiol Aging 35*, 793-801.

[69] Dinarello, C. A., Simon, A., and van der Meer, J. W. (2012) Treating inflammation by blocking interleukin-1 in a broad spectrum of diseases, *Nat Rev Drug Discov 11*, 633-652.

[70] Larsen, C. M., Faulenbach, M., Vaag, A., Ehses, J. A., Donath, M. Y., and Mandrup-Poulsen, T. (2009) Sustained effects of interleukin-1 receptor antagonist treatment in type 2 diabetes, *Diabetes Care 32*, 1663-1668.

[71] Westwell-Roper, C., Dai, D. L., Soukhatcheva, G., Potter, K. J., van Rooijen, N., Ehses, J. A., and Verchere, C. B. (2011) IL-1 blockade attenuates islet amyloid polypeptide-induced proinflammatory cytokine release and pancreatic islet graft dysfunction, *J Immunol 187*, 2755-2765.

[72] Coll, R. C., Robertson, A. A., Chae, J. J., Higgins, S. C., Munoz-Planillo, R., Inserra, M. C., Vetter, I., Dungan, L. S., Monks, B. G., Stutz, A., Croker, D. E., Butler, M. S., Haneklaus, M., Sutton, C. E., Nunez, G., Latz, E., Kastner, D. L., Mills, K. H., Masters, S. L., Schroder, K., Cooper, M. A., and O'Neill, L. A. (2015) A small-molecule inhibitor of the NLRP3 inflammasome for the treatment of inflammatory diseases, *Nat Med 21*, 248-255.

[73] Kapurniotu, A., Buck, A., Weber, M., Schmauder, A., Hirsch, T., Bernhagen, J., and Tatarek-Nossol, M. (2003) Conformational restriction via cyclization in β-amyloid peptide Aβ(1-28) leads to an inhibitor of Aβ(1-28) amyloidogenesis and cytotoxicity, *Chem Biol 10*, 149-159.

[74] Kazantzis, A., Waldner, M., Taylor, J. W., and Kapurniotu, A. (2002) Conformationally constrained human calcitonin (hCt) analogues reveal a critical role of sequence 17-21 for the oligomerization state and bioactivity of hCt, *Eur J Biochem 269*, 780-791.

[75] Kayed, R., Bernhagen, J., Greenfield, N., Sweimeh, K., Brunner, H., Voelter, W., and Kapurniotu, A. (1999) Conformational transitions of islet amyloid polypeptide (IAPP) in amyloid formation in vitro, *J Mol Biol 287*, 781-796.

[76] Asare, Y., Ommer, M., Azombo, F. A., Alampour-Rajabi, S., Sternkopf, M., Sanati, M., Gijbels, M. J., Schmitz, C., Sinitski, D., Tilstam, P. V., Lue, H., Gessner, A., Lange, D., Schmid, J. A., Weber, C., Dichgans, M., Jankowski, J., Pardi, R., de Winther, M. P., Noels, H., and Bernhagen, J. (2017) Inhibition of atherogenesis by the COP9 signalosome subunit 5 in vivo, *Proc Natl Acad Sci U S A 114*, E2766-E2775.

[77] Duewell, P., Kono, H., Rayner, K. J., Sirois, C. M., Vladimer, G., Bauernfeind, F. G., Abela, G. S., Franchi, L., Nunez, G., Schnurr, M., Espevik, T., Lien, E., Fitzgerald, K. A., Rock, K. L., Moore, K. J., Wright, S. D., Hornung, V., and Latz, E. (2010) NLRP3 inflammasomes are required for atherogenesis and activated by cholesterol crystals, *Nature 464*, 1357-1361.

[78] Boonacker, E., Elferink, S., Bardai, A., Fleischer, B., and Van Noorden, C. J. (2003) Fluorogenic substrate [Ala-Pro]2-cresyl violet but not Ala-Pro-rhodamine 110 is cleaved specifically by DPPIV activity: a study in living Jurkat cells and CD26/DPPIV-transfected Jurkat cells, *J Histochem Cytochem 51*, 959-968.

[79] Bernhagen, J., Krohn, R., Lue, H., Gregory, J. L., Zernecke, A., Koenen, R. R., Dewor, M., Georgiev, I., Schober, A., Leng, L., Kooistra, T., Fingerle-Rowson, G., Ghezzi, P., Kleemann, R., McColl, S. R., Bucala, R., Hickey, M. J., and Weber, C. (2007) MIF is a noncognate ligand of CXC chemokine receptors in inflammatory and atherogenic cell recruitment, *Nat Med 13*, 587-596.

FIGURE LEGENDS

Figure 1. IAPP-GI prevents Aβ40(42) and IAPP aggregate-induced NLRP3 inflammasome activation. (a) IAPP-GI blocks Aβ40- and IAPP-induced NLRP3 activation in LPS-primed BV-2 mouse microglial cells. Following LPS priming (100 ng/ml), cells were incubated overnight with 4-day-aged Aβ40 (10 µM), Aβ40+IAPP-GI (10 µM each), IAPP, IAPP+IAPP-GI (10 µM each), IAPP-GI alone, or ATP (1 mM) as indicated. NLRP3 activation was measured by caspase-1 activity (using the fluorescent cell-permeable FLICA substrate. (b) Same as (a) except that unprimed BV-2 microglial cells were used. This experiment also shows that IAPP-GI blocks Aβ42-induced NLRP3 activation. Results are means (±SEM) of 3-4 independent experiments with 7-10 replicates each. (c) Proof that inhibitory effect is dependent on NLRP3. Immortalized peritoneal macrophages (PMs) were primed with LPS and inhibition of Aβ40- or IAPP-induced caspase-1 activation by IAPP-GI is compared between wildtype (WT) and *Nlrp3* knockout (*Nlrp3*$^{-/-}$) cells. Incubation conditions as in (a), except that IAPP and IAPP-GI were applied at 5 µM each. (d) IAPP-GI prevents Aβ40(42) and IAPP aggregate-induced NLRP3 inflammasome activation in BV-2 microglia and peritoneal macrophages (PM) as measured by IL-1β production via ELISA from the cell supernatants. For PMs, wildtype (PM-WT) and *Nlrp3* knockout (PM-*Nlrp3*$^{-/-}$) cells were compared (triplicate measurements from a representative experiment). (e) Induction of caspase-1 activation in bone marrow-derived macrophages (BMDMs) by IAPP aggregates and inhibition by IAPP-GI. Cells were primed with LPS and treated with the peptides as in (a). Results (c) and (e) are means (±SEM) of 3-13 independent experiments each.

Figure 2. IAPP-GI inhibits Aβ40-induced cathepsin B activation and protects lysosomal integrity. BV-2 microglial cells were incubated with 4-day-aged Aβ40, Aβ+IAPP-GI (1/1) or IAPP-GI alone (10 µM) for 16 h and cathepsin B activity visualized with Magic red substrate (a). Data are means (±SEM) of three independent experiments. (b) Anti-cathepsin B Western blot (WB) of the lysosomal fraction isolated from BV-2 cells following incubation with Aβ40 alone, Aβ40+IAPP-GI or control buffer. (c) LAMP-1 signal (WB) verifies the lysosomal character of the isolated compartment.

Figure 3. Aβ40/IAPP-GI hetero-oligomers are internalized by microglial cells, targeted to lysosomal compartments and efficiently degraded. Confocal microscopy of microglial cells after overnight

incubation (16 h) with 200 nM of Fluos-Aβ40 (a), Fluos-IAPP-GI (b), or Fluos-Aβ40 + unlabeled IAPP-GI (c). (d) Lysosomal co-targeting of Rhodamin-Aβ40/Fluos-IAPP (200 nM each) hetero-oligomers. LysoTracker Red was used for lysosomal/late endosomal co-staining. Scale bars: 10 μm. (e) Enhanced elimination of Aβ40 from lysosomes in the context of its IAPP-GI hetero-oligomers. Aged Aβ40, Aβ40+IAPP-GI (1/1), or IAPP-GI were added to BV-2 cells (final concentration 10 μM) and incubated for 0, 2 and 16 h. Lysosomes were isolated and Aβ40 or IAPP-GI were quantified by WB with anti-Aβ40 (*left panel*) or anti-IAPP antibody (*right panel*).

Figure 4. Specificity of the interaction of IAPP-GI with Aβ40 and the IAPP sequence *per se* in inhibition of Aβ-mediated inflammasome activation – evidence for a predominant role of IAPP-GI/Aβ complexes in lysosomal trafficking, degradation, and protection over mere protection from Aβ-aggregation. (a) Interaction of IAPP-GI with non-fibrillar Aβ40 is required for IAPP-GI-mediated lysosomal Aβ40 degradation. IAPP-GI was added to 4 day-aged, fibrillar Aβ40 (10 μM; 1/1) and the solution was applied to BV-2 cells. Aged, fibrillar Aβ40 alone was also applied to the cells as control. Anti-Aβ40-Western blot (control: anti-IAPP) of enriched lysosomal fraction is shown. The blot shown is representative of 2-3 independent incubations. (b) Coincubation of Aβ40 with glucagon does not affect lysosomal degradation of Aβ40. 4 day-aged Aβ40 alone versus an aged Aβ40+glucagon mixture (1/1) were added to BV-2 cells at 10 μM and lysosomal fractions were analyzed by anti-Aβ40-WB. The blot shown is representative of 2-3 independent incubations. (c-d) The inhibitors of Aβ40 amyloidogenesis LPFFD and EGCG do not promote lysosomal degradation of Aβ40. Methods and detection are as in (b). The blots shown are representative of 3-4 independent incubations. (e-f) Non-amyloidogenic rIAPP, a highly potent IAPP receptor agonist, strongly enhances lysosomal Aβ40 degradation and blocks caspase-1 activation. Methods are as in (b), except that in addition, a FLICA substrate-based caspase-1 activation assay was performed. The blot is representative of 2-3 independent incubations and the caspase-1 activity data are means ±SEM of 3 independent experiments. (g-h) Non-fibrillar Aβ40/IAPP hetero-oligomers are targeted to lysosomes, promote degradation of both polypeptides and inhibit caspase-1 activation mediated by Aβ40 and IAPP. Methods are as in (e-f). Data are means (±SEM) of three independent experiments.

Figure 5. Cellular uptake of Aβ40/IAPP-GI and IAPP/IAPP-GI hetero-oligomers is mediated by a rapid IAPP receptor-mediated endocytosis pathway. (a) Formation of Aβ40/IAPP-GI hetero-oligomers promotes rapid disappearance of Aβ40 from BV-2 cell supernatant. 4-day-aged fibrillar Aβ40 alone or Aβ40/IAPP-GI mixtures were added to BV-2 cells at 10 μM. After 2 min and 16 h of incubation, supernatants were analyzed by Western blot for Aβ40. The blot is representative of 3 independent incubations. (b) Quantification of (a) by band densitometry with normalization to Aβ40 band alone at 2 min. Data are means ±SEM of 3 independent experiments. (c) Aβ40 in hetero-oligomeric complex with IAPP-GI is rapidly endocytosed by BV2 microglial cells. Dependency of uptake on a clathrin- and dynamin-dependent process. After treating BV2 cells with monodansylcadaverin (MDC) (50 μM) and Dynasore (80 μM), 4 day-aged peptides were added to the cells and incubated for 2, 30 and 60 min. The level of endocytosed Aβ40 or Aβ40+IAPP-GI hetero-complex was analyzed by Western blotting of cell lysates with anti-Aβ40 antibody (see Supplementary Figure S7 for blot image). Quantification of Western blot by band densitometry. Peptide control (input): 5 μg Aβ40 and Aβ40+IAPP-GI (1:1). Aβ monomer bands were normalized to input and actin. Data are means ±SEM of three independent experiments. (d) BV-2 cells express functional IAPP receptors. Radioactive receptor competition assay using ^{125}I-rIAPP as tracer and IAPP or IAPP-GI as competing agonist. Data are means (±SEM) of at least 3 independent experiments; *P<0.05, **P<0.001 and ***P<0.0001 versus tracer alone. (e) Same as (d) except that Aβ40/IAPP-GI (1/1) hetero-oligomers were used for competition. For comparison, binding of Aβ40 alone (5 μM) was also tested. (f) BV-2 cells express the IAPP receptor subtype AMY3. Cells were lysed and CTR and RAMP3 detected by Western blot. (g) Receptor targeting and lysosomal degradation by hetero-complexation with IAPP-GI extends to aged IAPP aggregates. Aged IAPP alone versus coincubation with IAPP-GI were added to bone marrow-derived macrophages (BMDMs) at 2 μM and incubated for 2 and 16 h. Upon isolation of lysosomal compartments, degradation was probed by Western blot with an anti-IAPP antibody. The Western blot shown is representative of 2 (2 h-time point) and 4 (16 h-time point) independent experiments. The IAPP monomer is indicated by an arrow. (h) Quantification of the Western blots according to (g). The IAPP monomer bands were quantitated. The 16 h-data are derived from 4 independent experiments, the 2 h-data refer to 2 independent experiments.

Figure 6. Cartoon summarizing the results and suggested “dual-hit” inhibitory mechanism of IAPP-GI on Aβ40-aggregate mediated microglial inflammation.

Figures

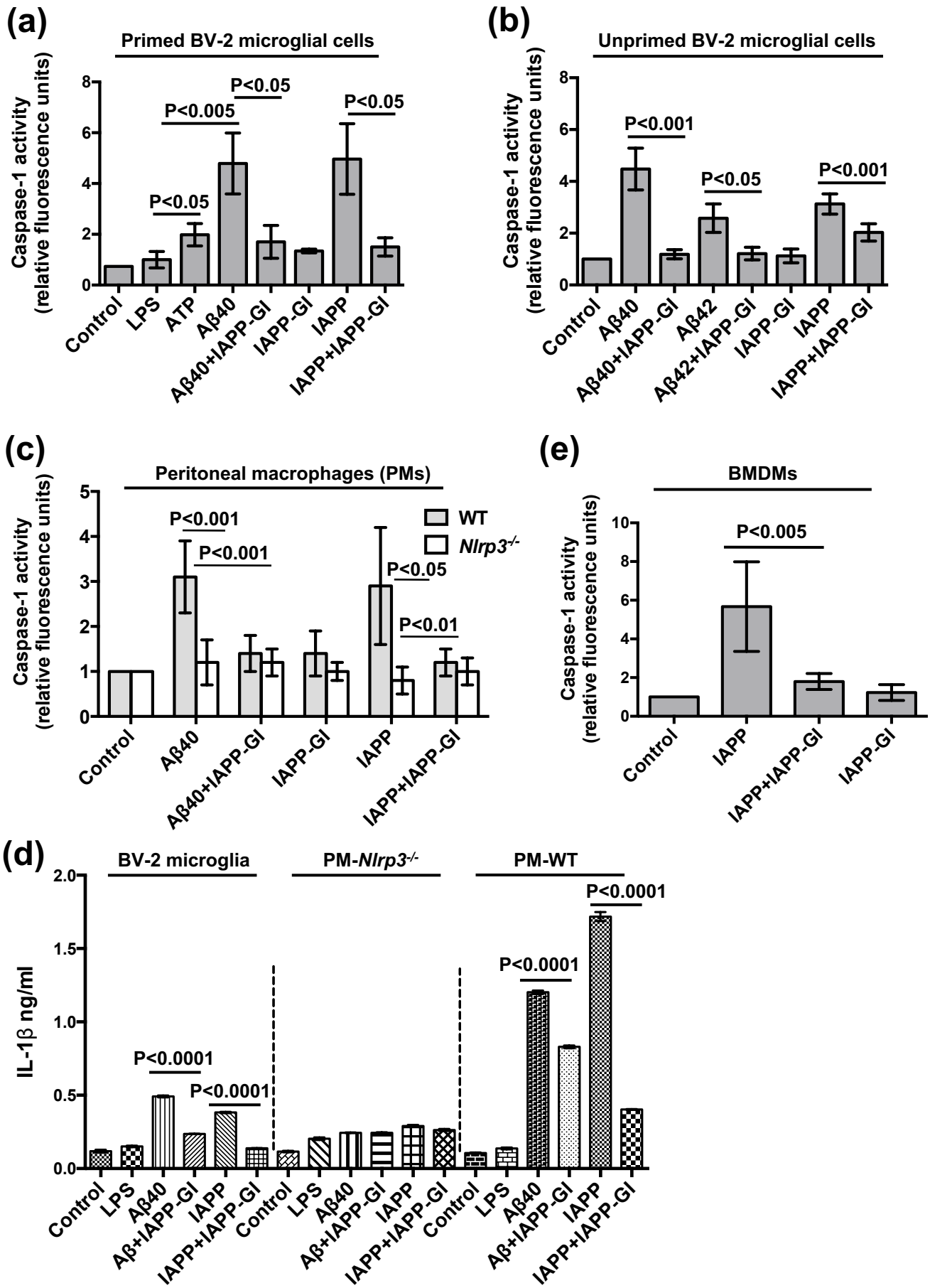
(a)
Primed BV-2 microglial cells
Caspase-1 activity (relative fluorescence units)
P<0.05
P<0.005
P<0.05
P<0.05
Control
LPS
ATP
Aβ40
Aβ40+IAPP-GI
IAPP-GI
IAPP
IAPP+IAPP-GI
(b)
Unprimed BV-2 microglial cells
Caspase-1 activity (relative fluorescence units)
P<0.001
P<0.05
P<0.001
Control
Aβ40
Aβ40+IAPP-GI
Aβ42
Aβ42+IAPP-GI
IAPP-GI
IAPP
IAPP+IAPP-GI
(c)
Peritoneal macrophages (PMs)
Caspase-1 activity (relative fluorescence units)
WT
Nlrp3-/-
P<0.001
P<0.001
P<0.05
P<0.01
Control
Aβ40
Aβ40+IAPP-GI
IAPP-GI
IAPP
IAPP+IAPP-GI
(e)
BMDMs
Caspase-1 activity (relative fluorescence units)
P<0.005
Control
IAPP
IAPP+IAPP-GI
IAPP-GI
(d)
BV-2 microglia
PM-Nlrp3-/-
PM-WT
IL-1β ng/ml
P<0.0001
P<0.0001
P<0.0001
P<0.0001
Control
LPS
Aβ40
Aβ+IAPP-GI
IAPP
IAPP+IAPP-GI

Figure 2; Aftabizadeh et al., 2019

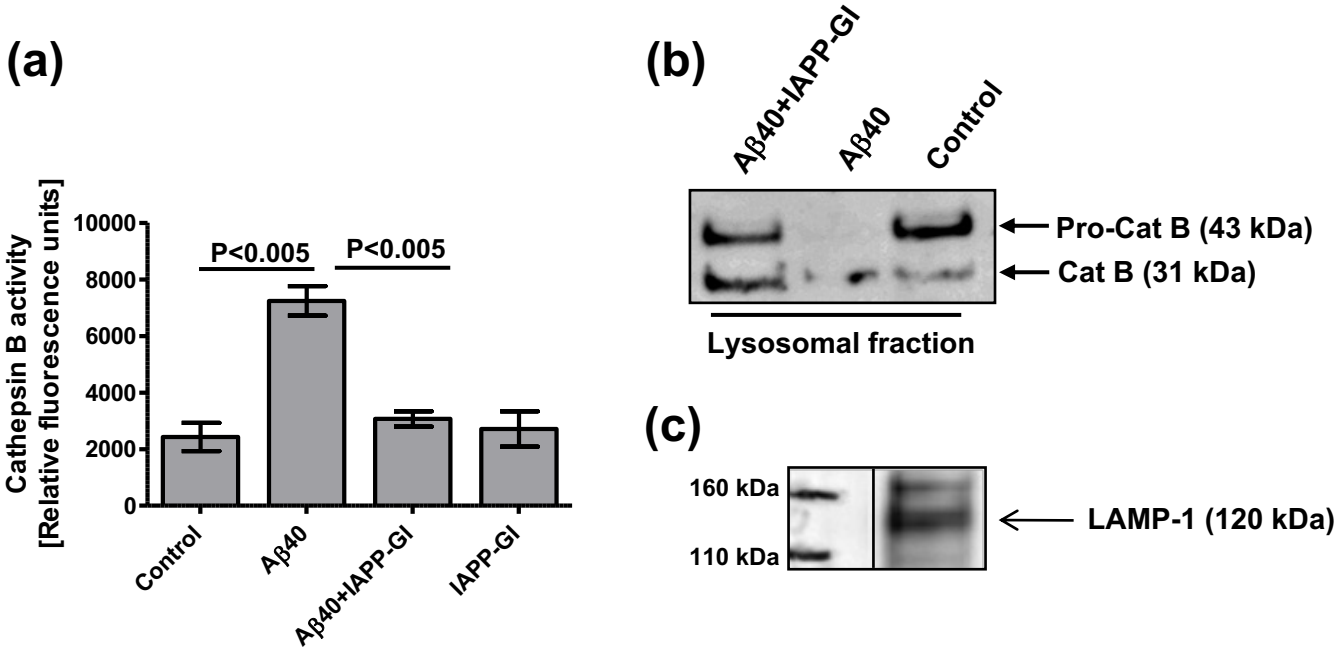

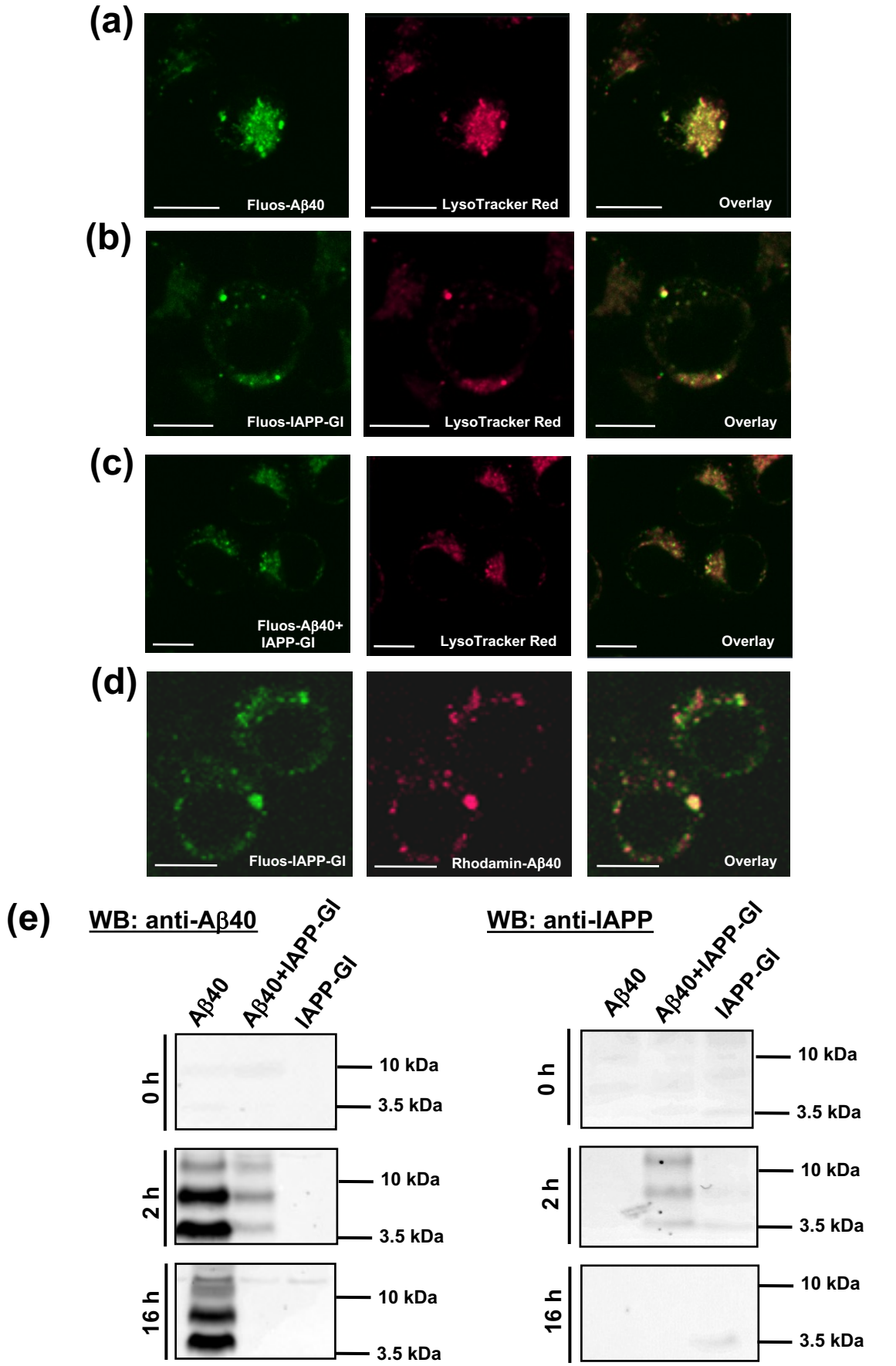
(a)
Fluos-Aβ40
LysoTracker Red
Overlay
(b)
Fluos-IAPP-GI
LysoTracker Red
Overlay
(c)
Fluos-Aβ40+
IAPP-GI
LysoTracker Red
Overlay
(d)
Fluos-IAPP-GI
Rhodamin-Aβ40
Overlay
(e)
WB: anti-Aβ40
Aβ40
Aβ40+IAPP-GI
IAPP-GI
0 h
2 h
16 h
10 kDa
3.5 kDa
WB: anti-IAPP
Aβ40
Aβ40+IAPP-GI
IAPP-GI
0 h
2 h
16 h
10 kDa
3.5 kDa

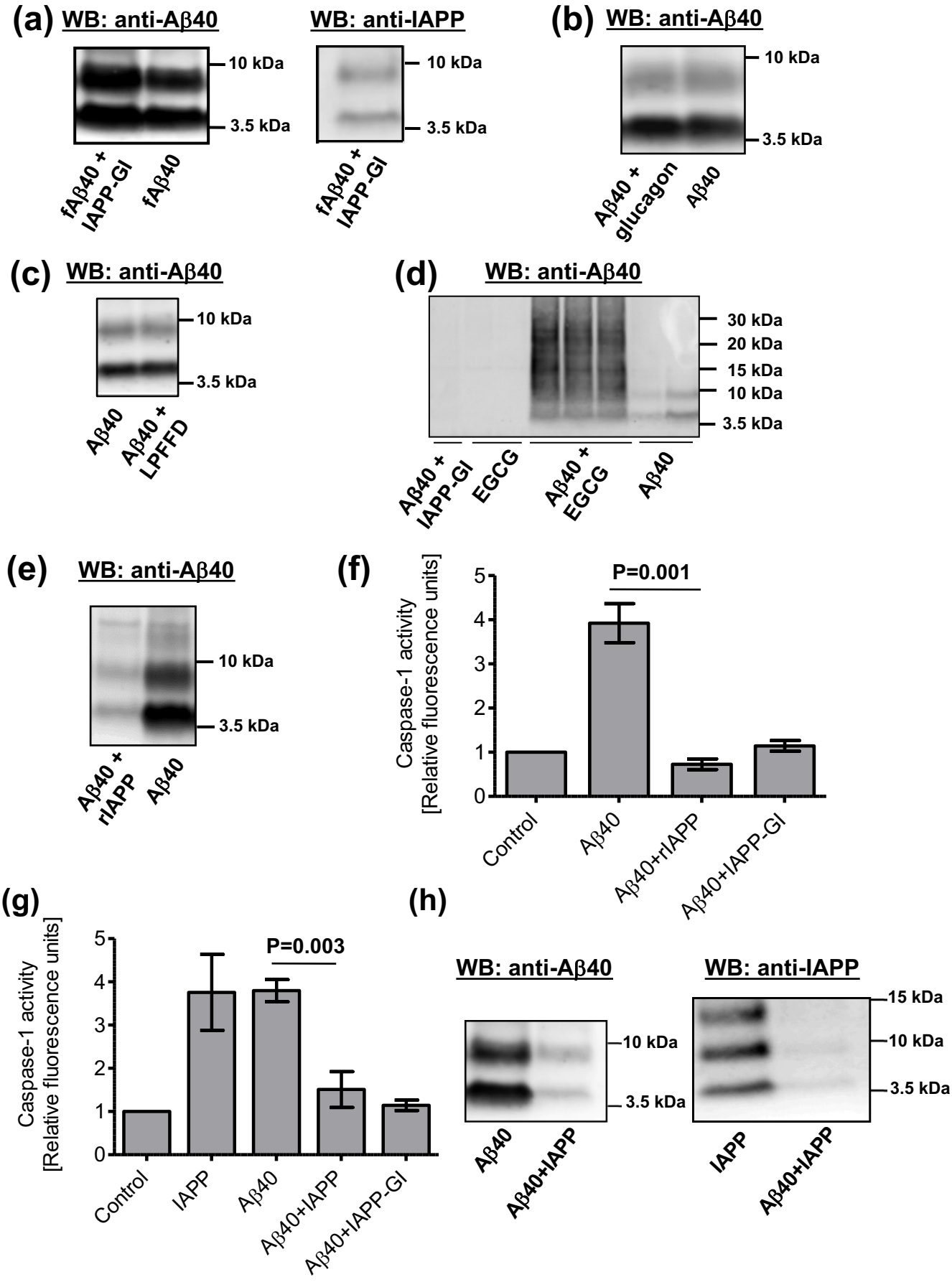
(a)
WB: anti-Aβ40
10 kDa
3.5 kDa
fAβ40 + IAPP-GI
fAβ40
WB: anti-IAPP
10 kDa
3.5 kDa
fAβ40 + IAPP-GI
(b)
WB: anti-Aβ40
10 kDa
3.5 kDa
Aβ40 + glucagon
Aβ40
(c)
WB: anti-Aβ40
10 kDa
3.5 kDa
Aβ40
Aβ40 + LPFFD
(d)
WB: anti-Aβ40
30 kDa
20 kDa
15 kDa
10 kDa
3.5 kDa
Aβ40 + IAPP-GI
EGCG
Aβ40 + EGCG
Aβ40
(e)
WB: anti-Aβ40
10 kDa
3.5 kDa
Aβ40 + rIAPP
Aβ40
(f)
Caspase-1 activity [Relative fluorescence units]
P=0.001
0
1
2
3
4
5
Control
Aβ40
Aβ40+rIAPP
Aβ40+IAPP-GI
(g)
Caspase-1 activity [Relative fluorescence units]
P=0.003
0
1
2
3
4
5
Control
IAPP
Aβ40
Aβ40+IAPP
Aβ40+IAPP-GI
(h)
WB: anti-Aβ40
10 kDa
3.5 kDa
Aβ40
Aβ40+IAPP
WB: anti-IAPP
15 kDa
10 kDa
3.5 kDa
IAPP
Aβ40+IAPP

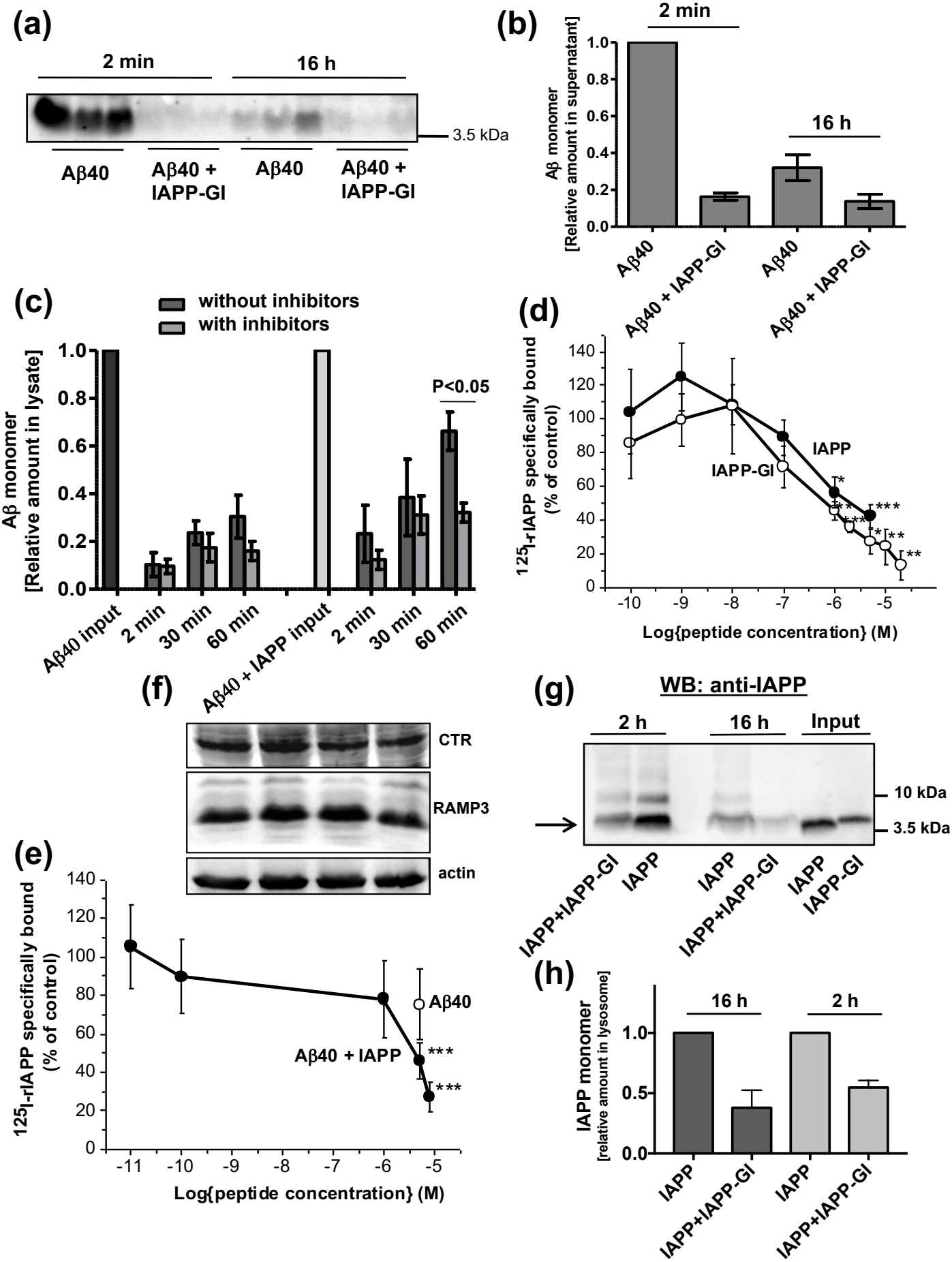
(a)
2 min
16 h
3.5 kDa
Aβ40
Aβ40 + IAPP-GI
Aβ40
Aβ40 + IAPP-GI
(b)
2 min
16 h
Aβ monomer [Relative amount in supernatant]
Aβ40
Aβ40 + IAPP-GI
Aβ40
Aβ40 + IAPP-GI
(c)
without inhibitors
with inhibitors
P<0.05
Aβ monomer [Relative amount in lysate]
Aβ40 input
2 min
30 min
60 min
Aβ40 + IAPP input
2 min
30 min
60 min
(d)
125I-rIAPP specifically bound (% of control)
IAPP
IAPP-GI
Log{peptide concentration} (M)
(e)
125I-rIAPP specifically bound (% of control)
Aβ40
Aβ40 + IAPP
Log{peptide concentration} (M)
(f)
CTR
RAMP3
actin
(g)
WB: anti-IAPP
2 h
16 h
Input
10 kDa
3.5 kDa
IAPP+IAPP-GI
IAPP
IAPP
IAPP+IAPP-GI
IAPP
IAPP-GI
(h)
16 h
2 h
IAPP monomer [relative amount in lysosome]
IAPP
IAPP+IAPP-GI
IAPP
IAPP+IAPP-GI

Figure 6; Aftabizadeh et al., 2019

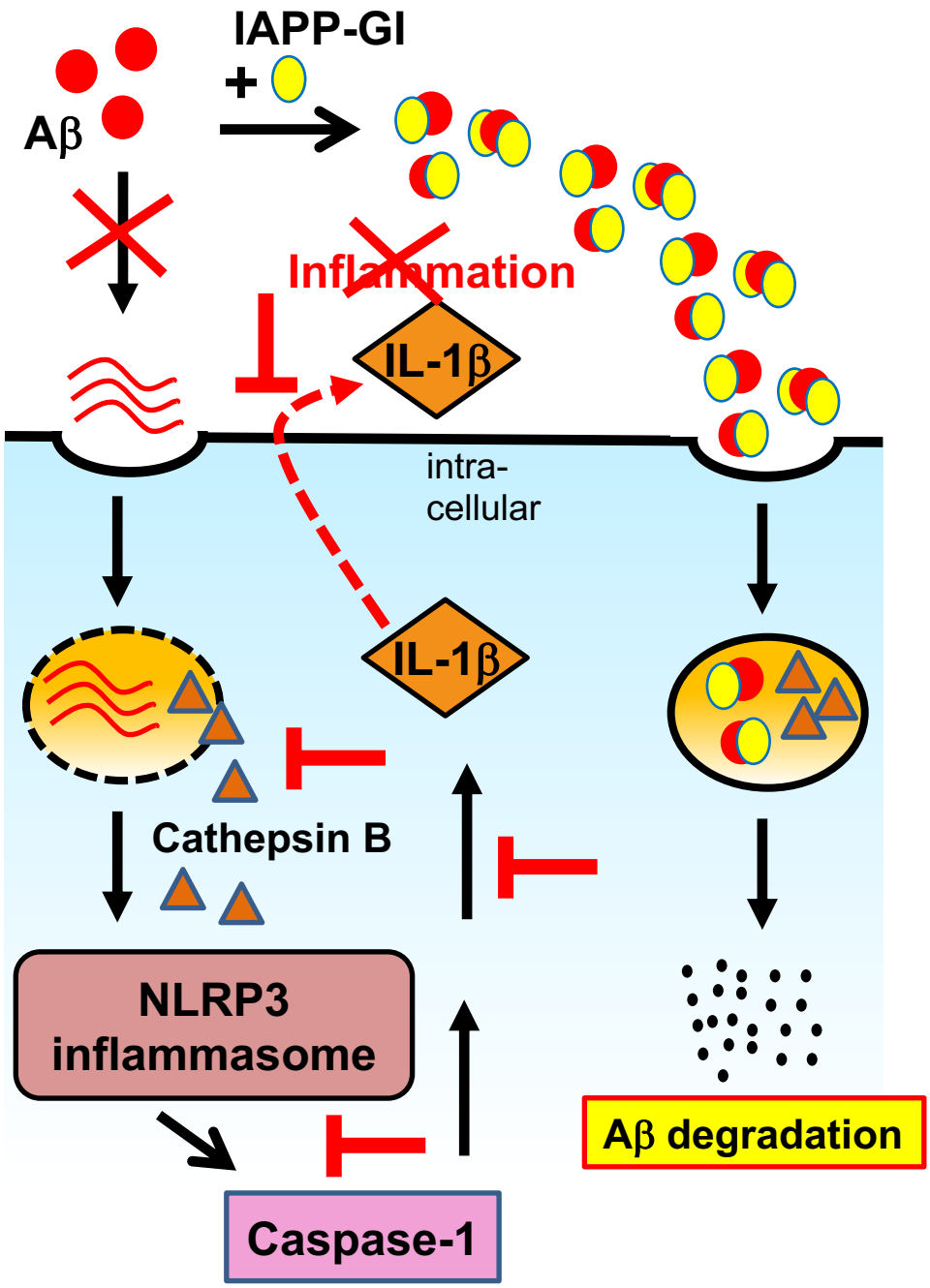

Supporting Information

Blocking inflammasome activation caused by β-amyloid peptide (Aβ) and islet amyloid polypeptide (IAPP) through an IAPP mimic

Maryam Aftabizadeh[1,2,3], Marianna Tatarek-Nossol[2], Erika Andreetto[1], Omar El Bounkari[4], Markus Kipp[5], Cordian Beyer[6], Eicke Latz[7,8], Jürgen Bernhagen[4,9*], and Aphrodite Kapurniotu[1*]

[1]Division of Peptide Biochemistry, Technische Universität München, Emil-Erlenmeyer-Forum 5, D-85354 Freising (Germany); [2]Institute of Biochemistry and Molecular Cell Biology and [6]Institute of Neuroanatomy, RWTH Aachen University, Pauwelsstr. 30, 52074 Aachen (Germany); [3]Cancer Immunotherapeutics and Tumor Immunology, City of Hope Medical Center Duarte, 1500 East Duarte Road, Duarte, CA 91010-3000 (USA); [4]Chair of Vascular Biology, Institute for Stroke and Dementia Research, Klinikum der Universität München, Ludwig-Maximilians-University of Munich, 81377 Munich (Germany); [5]Department of Anatomy II, Ludwig-Maximilians-University of Munich, 80336 Munich (Germany); [7]Institute of Innate Immunity, University of Bonn, Biomedical Center, University of Bonn, Sigmund-Freud-Str. 25, 53127 Bonn (Germany); [8]University of Massachusetts Medical School, Division of Infectious Diseases & Immunology, 364 Plantation St., Worcester, MA 01605 (USA); [9]Munich Cluster for Systems Neurology (SyNergy), 81377 Munich (Germany).

Figure S1

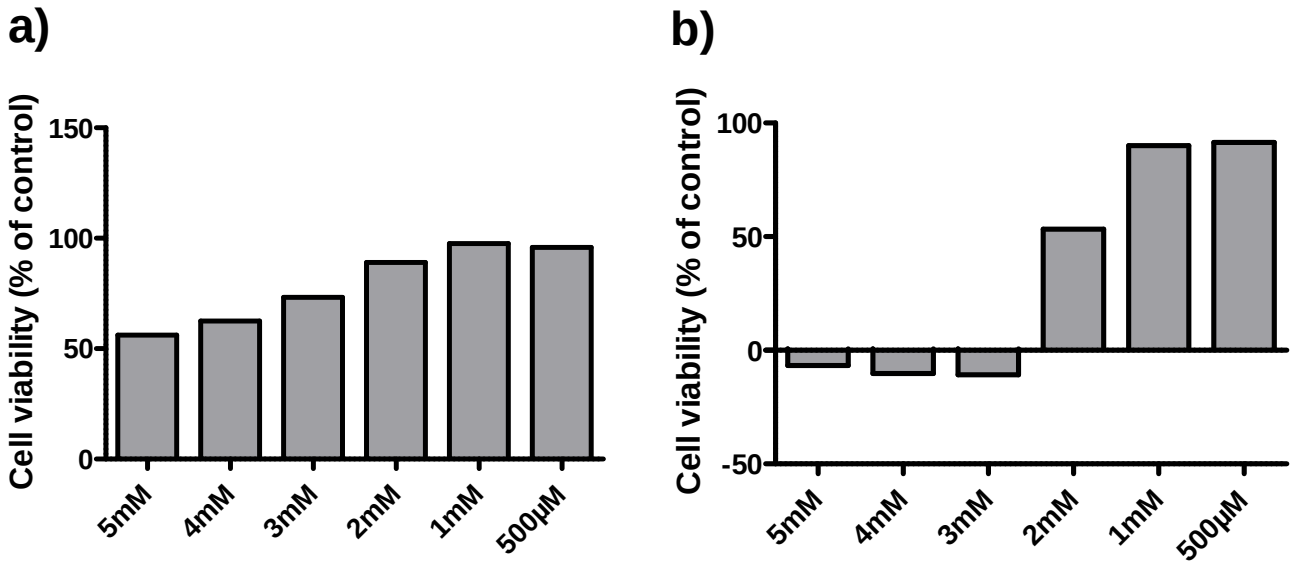

Figure S1. One mM ATP does not impair viability of BV2 microglial cells. The potential cytotoxicity of ATP on cell viability of BV2 was assessed by MTT cell viability/metabolic activity assay. Titration of different concentrations of ATP (0.5 - 5 mM). BV2 cells were incubated with ATP for 30 min (a) or 18 h (b). Appreciable cytotoxic effects of ATP were only seen at concentrations ≥2 mM. 1 mM and 500 µM ATP were not cytotoxic.

Figure S2

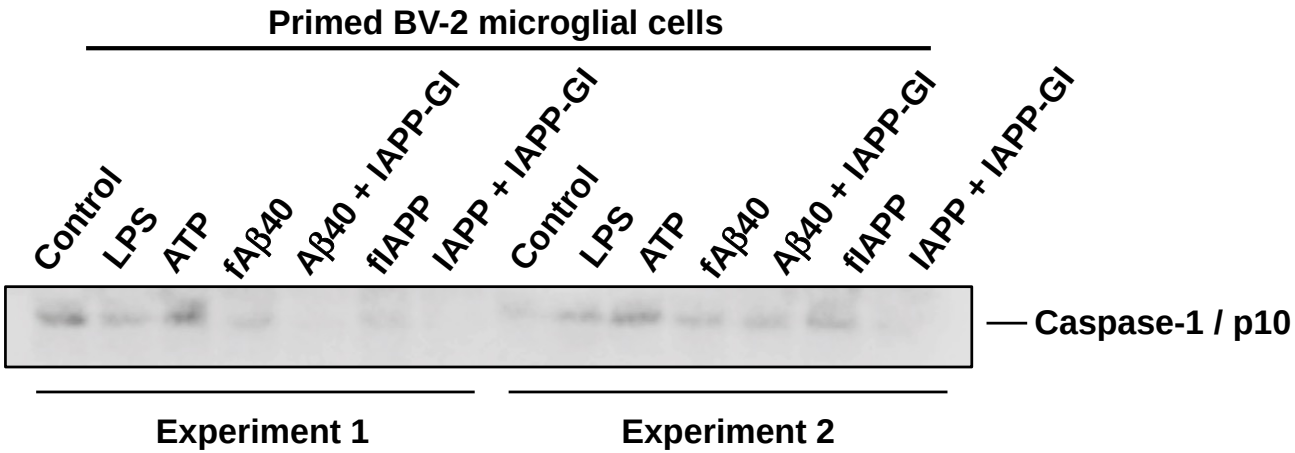

Figure S2. NLRP3 inflammasome activation in microglial cells by aged Aβ40 or IAPP as detected by autoproteolytic generation of caspase-1 subunit p10 and blockade by IAPP-GI. 4 day-aged solutions of Aβ40 versus Aβ40+IAPP-GI or IAPP versus IAPP+IAPP-GI were added to LPS-primed BV-2 microglial cells at a final peptide concentration of 10 µM peptide as indicated. Controls: unprimed cells (control); LPS priming without second hit trigger (LPS); LPS priming + ATP as surrogate second hit trigger (ATP). Caspase-1 subunit p10, indicating activation and autoproteolytic cleavage of caspase-1, was detected by Western blot. Two independent experiments were performed.

Figure S3

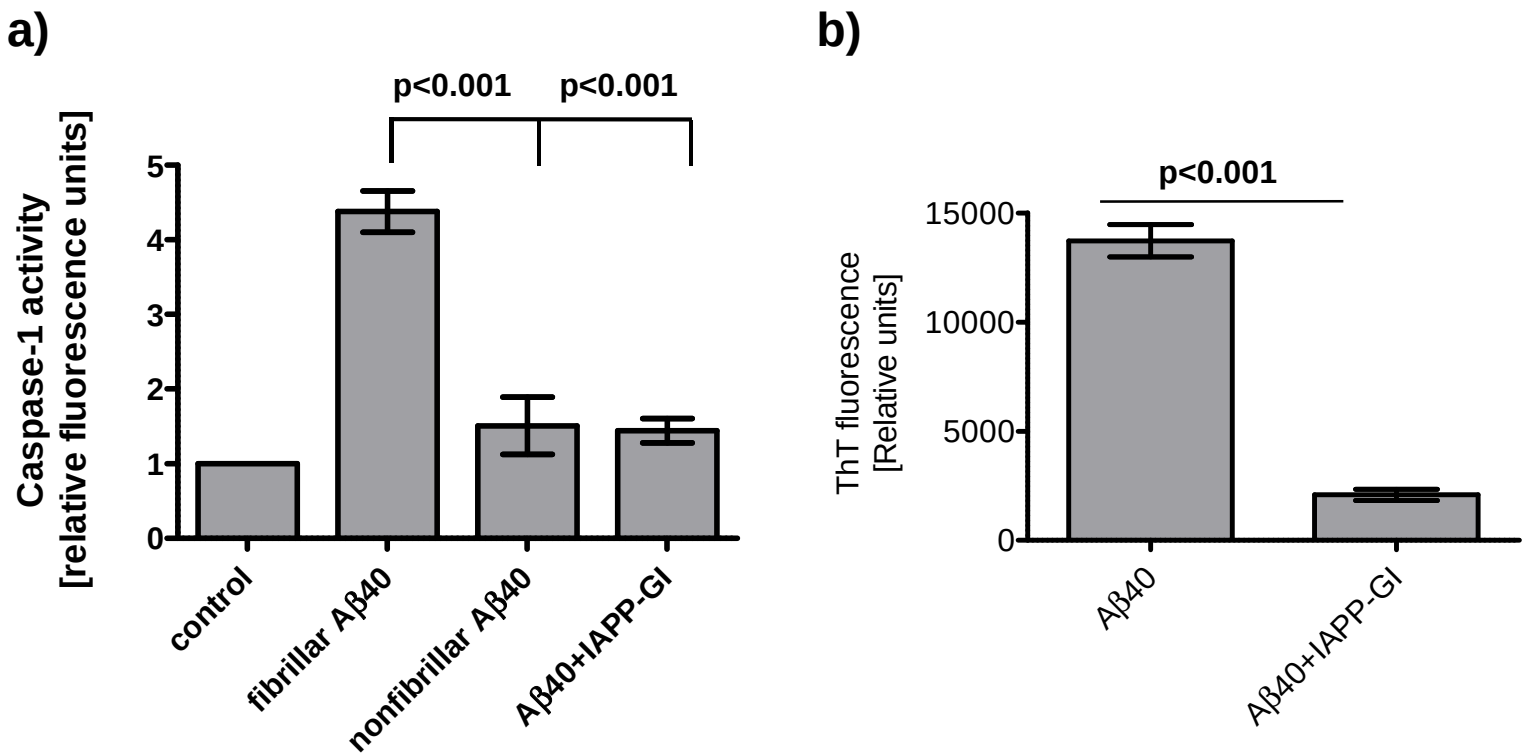

Figure S3. Nonfibrillar Aβ40 does not activate NALP3 inflammasome activity and verification of Aβ40 fibril formation. a) Nonfibrillar Aβ40 does not activate caspase-1 in BV2 microglial cells. Aβ40 as well as Aβ40+IAPP-GI were dissolved in 50 mM sodium phosphate buffer, containing 100 mM NaCl plus 1% HFIP with a pH value of 7.4, to a concentration of 100 µM and incubated at room temperature for 4 days and then were added to BV2 microglial cells at a final peptide concentration of 10 µM. Shortly before stimulation, nonfibrillar Aβ40 was also dissolved in 50 mM sodium phosphate buffer, containing 100 mM NaCl plus 1% HFIP with a pH value of 7.4, to a concentration of 100 µM and added to the cells (without preincubation) to a final concentration of 10 µM on the cells. All samples were incubated overnight (16 h) with the cells. Caspase-1 activation was measured by incubation with a fluorescent cell-permeable substrate (FLICA) that binds only to activated caspase-1. Results are means ±SEM of 4-10 independent experiments. b) Verification of Aβ40 fibril formation and inhibition by IAPP-GI. Before applying to the cells, fibril formation was measured by ThT binding assay. Results are means ±SEM of three independent experiments.

Figure S4

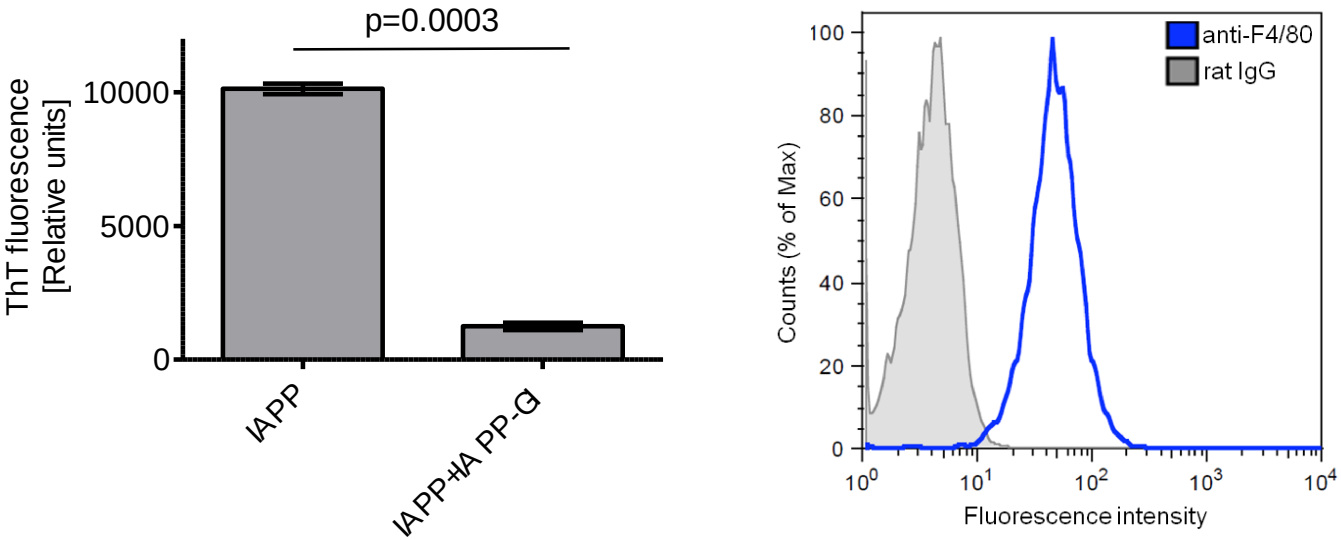

Figure S4. Verification of bone marrow-derived macrophage differentiation and inhibition of IAPP fibrillation by IAPP-GI. a) Flow cytometry analysis detecting F4/80 expression shows differentiation of bone marrow-derived macrophages (BMDMs). Rat IgG was used as a control antibody. b) IAPP-GI blocks IAPP fibril formation. IAPP fibrillation was analyzed by Thioflavin T binding assay before applying peptides to BMDMs. Results are means ±SEM of three independent experiments.

Figure S5

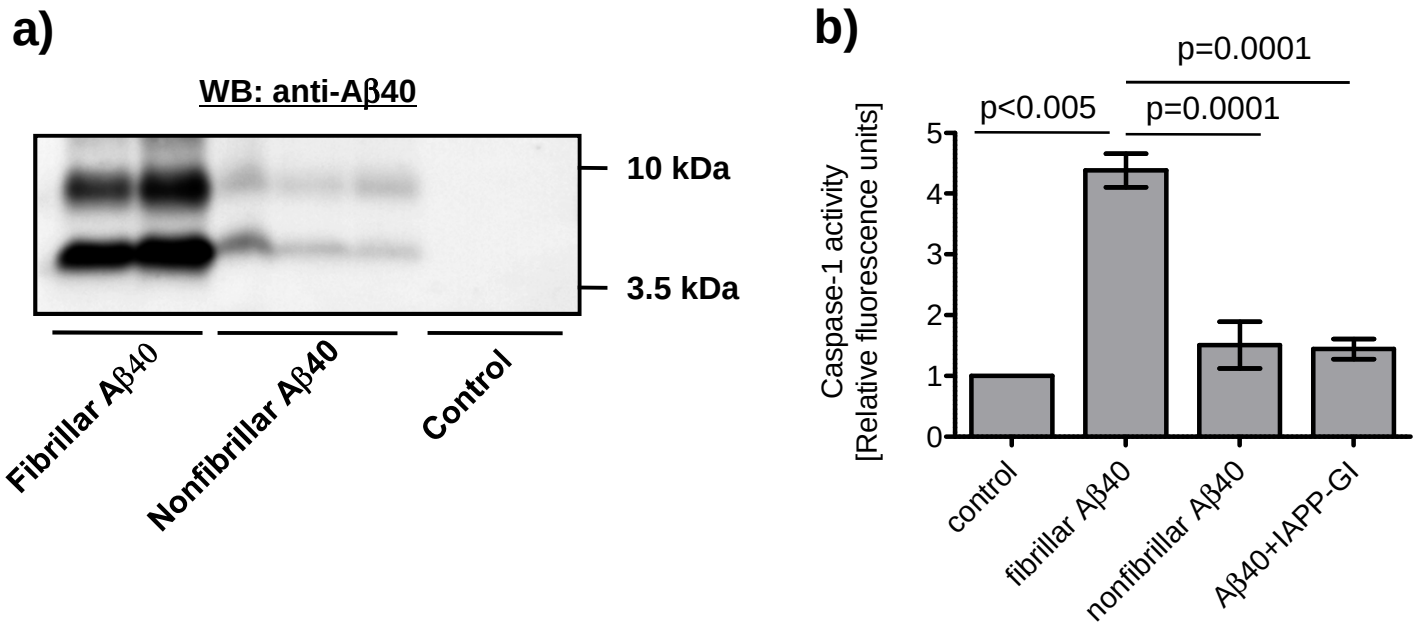

***Figure S5*.** Non-aggregated Aβ40 is rapidly degraded in lysosomes and does not activate caspase-1. a) Nonfibrillar Aβ40 disappears more rapidly from lysosomes than fibrillar Aβ40. Aβ40 was dissolved in 50 mM sodium phosphate buffer, containing 100 mM NaCl plus 1% HFIP with a pH value of 7.4 at a concentration of 100 µM and incubated at room temperature for 4 days and was termed fibrillar Aβ40. Shortly before adding fibrillar Aβ40 to BV-2 microglial cells, nonfibrillar Aβ40 was also dissolved in 50 mM sodium phosphate buffer, containing 100 mM NaCl plus 1% HFIP with a pH value of 7.4 (concentration: 100 µM). Both fibrillar and nonfibrillar Aβ40 were then added to the cells at a final concentration of 10 µM. Buffer was used as a further control. Incubations were for 16 h. Lysosomes were isolated and lysosomal extracts analyzed by Western blotting (for method see main manuscript text body). Non-fibrillar Aβ40 was substantially degraded with only weak bands detectable, whereas fibrillar Aβ40 was massively present, indicating protection from degradation. Fibrillar Aβ40 and control buffer were analyzed in duplicate, nonfibrillar Aβ40 in triplicate. b) Nonfibrillar Aβ40 does not activate caspase-1 in BV-2 microglial cells. Fibrillar Aβ40 was prepared as under a) and was also applied in a mixture (1:1) with IAPP-GI. BV-2 cells were incubated with the various Aβ preparations as indicated for 16 h and caspase-1 activity of cell lysates measured (see methods).

Figure S6

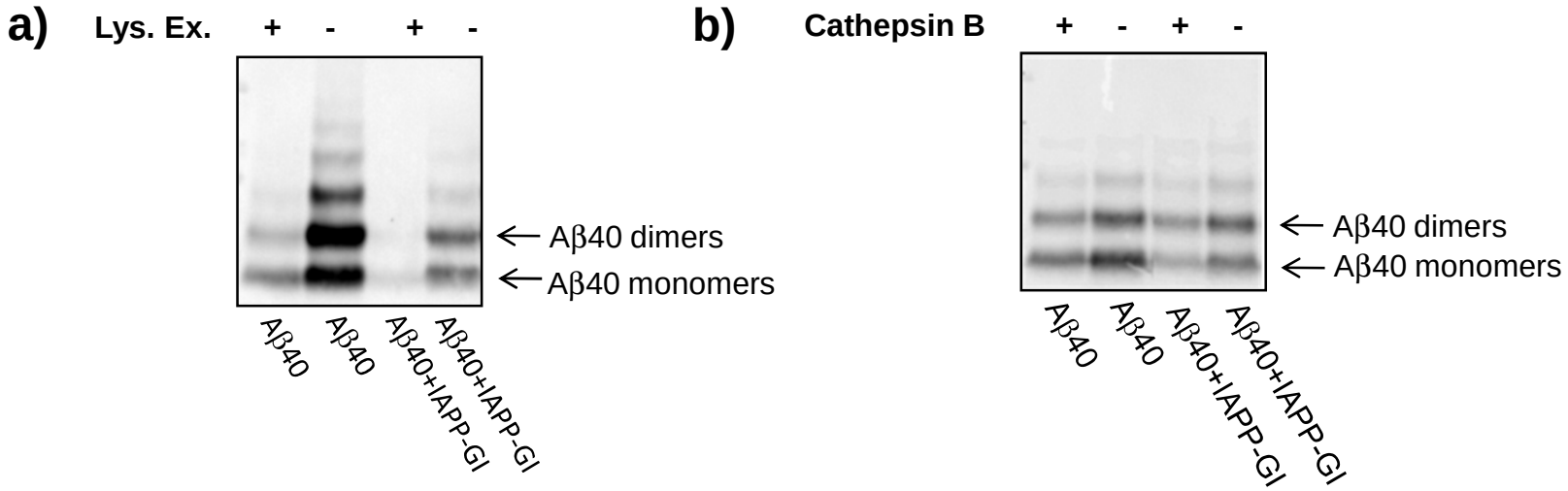

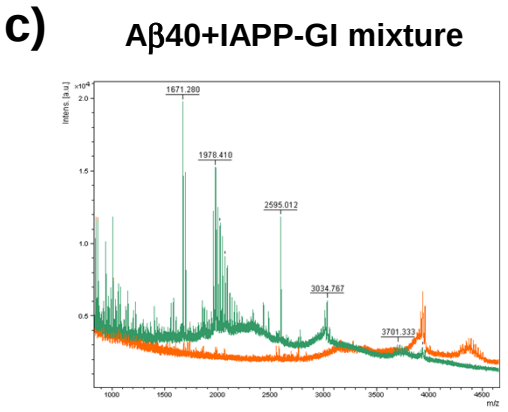

***Figure S6*.** Confirmatory evidence that lysosomal enzymes degrade Aβ40 within Aβ40/IAPP-GI hetero-oligomeric complexes. a) Western blot analysis (using anti-Aβ antibody) showing that lysosomal extracts lead to a more pronounced degradation of Aβ40 when present within Aβ40/IAPP-GI complexes compared to Aβ40 alone (compare the relative loss in Aβ40 signals in lane 3/4 versus 1/2). 100 µM Aβ40 versus Aβ40+IAPP-GI (1/1) (final concentrations 10 µM, pH value adjusted to 5) were incubated at room temperature for 4 days (“aging”), before subjecting preparations to isolated lysosomal extracts from BV-2 microglial cells for 16 h. b) Same as a) except that peptide preparations were incubated with purified commercial cathepsin B. Blots shown in a) and b) are representative of 2-3 independent experi-ments. c) MALDI-mass spectrometry analysis of the Aβ40/IAPP-GI hetero-oligomeric complexes digested with cathepsin B. As expected, the spectrum of undigested Aβ40/IAPP-GI complex shows signals at ≈3940 m/z (IAPP-GI) and ≈4350 m/z (Aβ40). Following digestion, these peaks have vanished and the spectrum of cathepsin B-digested Aβ40/IAPP-GI complex shows various peaks at lower masses.

Figure S7

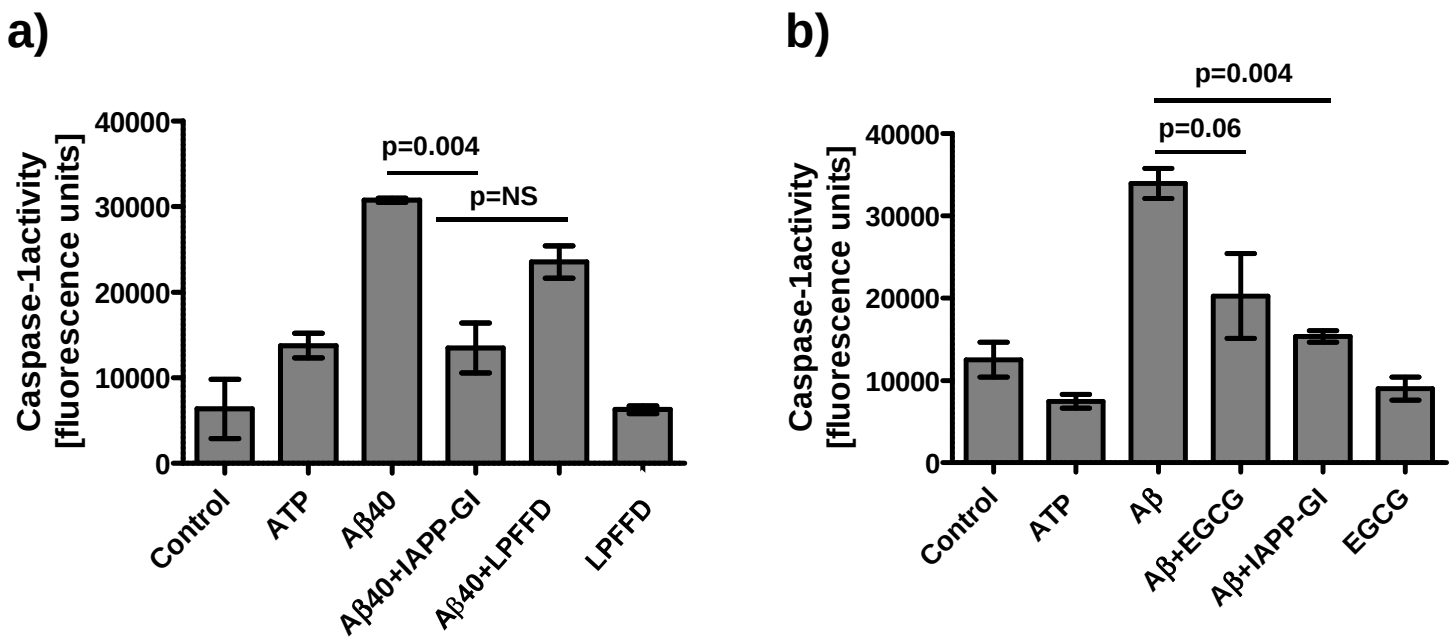

***Figure S7*.** Aβ40 aggregate-triggered NLRP3 inflammasome activation is not reduced by the small molecule amyloid inhibitors pentaptide LPFFD or green tea compound EGCG. Inflammasome activation in BV2 microglial cells was measured by caspase-1 activity assay. a) Aβ40 aggregate-triggered caspase-1 activation is not inhibited by anti-amyloidogenic pentapeptide LPFFD. Caspase-1 activation in BV2 cells was measured after stimulation with 1mM ATP, 10 μM fibrillar Aβ40 (4 day-aged), 10 μM aged Aβ40+IAPP-GI (1:1), and 10 μM Aβ40+LPFFD (1:1). b) same as a) except that instead of LPFFD, EGCG was applied. Data are means ±SEM of 3-6 independent experiments. Asterisks indicate statistical significance; NS = non-significant.

Figure S8

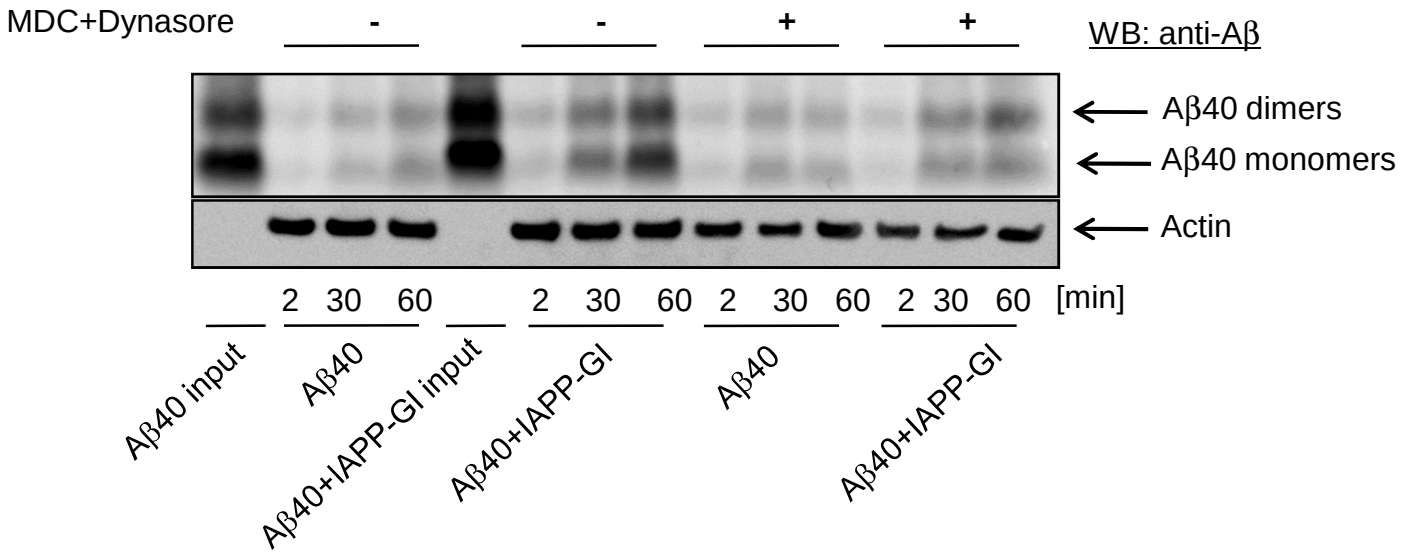

***Figure S8*.** Aβ40 in hetero-oligomeric complex with IAPP-GI is rapidly endocytosed by BV2 microglial cells. Dependency of uptake of the Aβ40+IAPP-GI hetero-complex on a clathrin- and dynamin-dependent process. After treating BV2 cells with monodansylcadaverin (MDC) (50 μM) and Dynasore (80 μM), 4 day-aged peptides were added to the cells and incubated for 2, 30 and 60 min. The level of endocytosed Aβ40 or Aβ40+IAPP-GI hetero-complex was analyzed by Western blotting of cell lysates with anti-Aβ40 antibody. The blot shown is representative of three independent experiments.

Figure S9

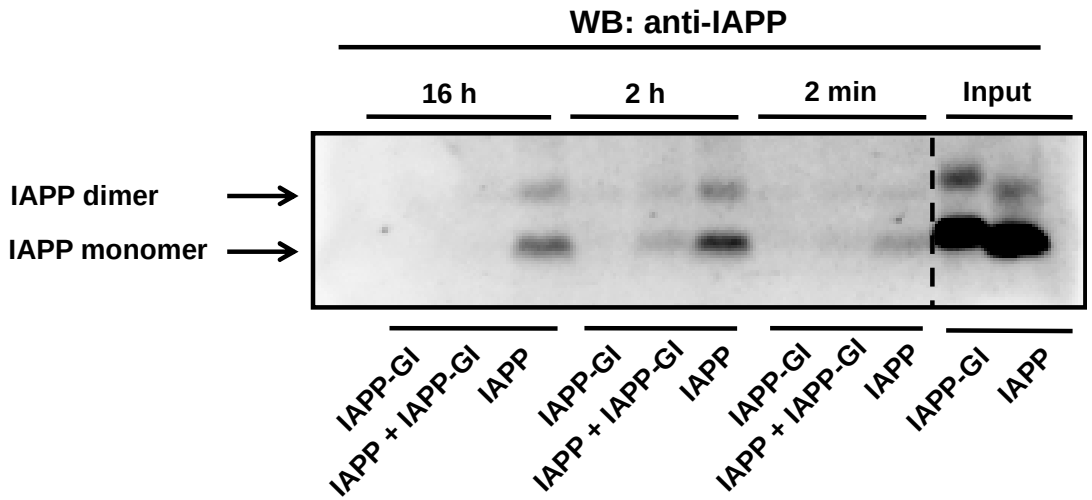

***Figure S9*.** Cellular uptake and lysosomal degradation of IAPP/IAPP-GI hetero-oligomers is mediated by a rapid IAPP receptor-mediated endocytosis pathway. Aged IAPP alone versus coincubations with IAPP-GI were added to bone marrow-derived macrophages (BMDMs) at 2 μM and incubated for 2 min, 2 h and 16 h. Upon isolation of lysosomal compartments, degradation was probed by Western blot with an anti-IAPP antibody. The IAPP monomer and dimer is indicated by an arrow. Input (500 ng per lane) indicates the amounts of IAPP and IAPP-GI added to the cell incubations and that the anti-IAPP antibody recognizes both IAPP and IAPP-GI, although IAPP-GI is recognized at slightly lower binding efficiency. The blot shown is representative of two (2 h), three (2 min) and four (16 h) independent experiments.